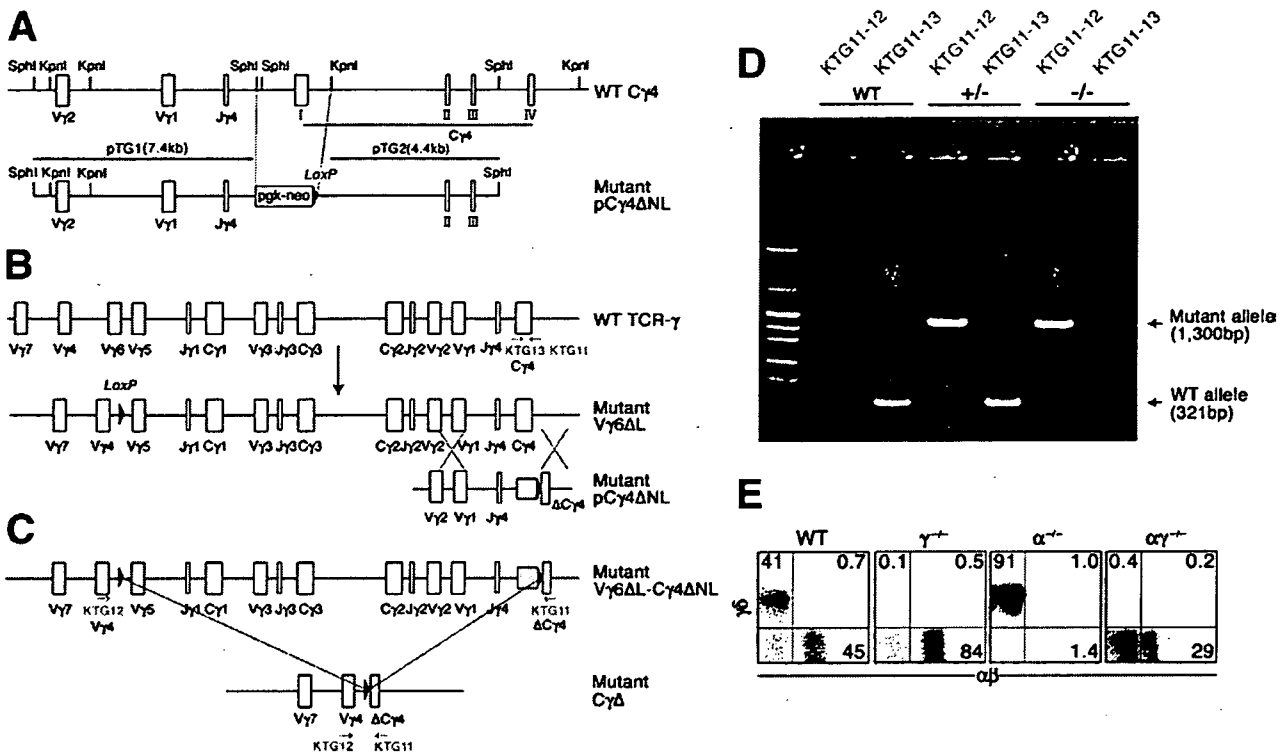

Figure 2. Generation of TCRγ-deficient mice and subsequent production of TCRαγ double mutant mice. (*A*) Schematic representation of WT and mutant (pCγ4ΔNL) genomic Cγ4 loci together with the 3 DNA fragments used to construct the mutant pCγ4ΔNL vector. The resulting targeting vector (pCγ4ΔNL) carrying a *loxP*-flanked *pgk-neo* gene cassette in place of exon 1 of Cγ4 gene used a neomycin resistance gene driven by the *pgk* promoter as positive selection marker is shown. Restriction enzyme sites, *Sph*I and *Kpn*I (*solid bars*), exon structures, Vγ and Jγ (*open boxes*), and *loxP* site (*solid triangle*) are indicated. (*B*) Schematic representation of the ES clone carrying WT TCRγ gene and mutant Vγ6ΔL ES clone carrying the allele in which the Vγ6 region was replaced by a single *loxP* site and mutant pCγ4ΔNL targeting vector. Exon structures, Vγ and Jγ (*open boxes*) and *loxP* site (*solid triangle*) are indicated. (*C*) Schematic representation of generation of the mutant mice that carry the TCRγ-deficient (CγΔ) allele by Cre-mediated recombination during embryonic development. Exon structures, Vγ and Jγ (*open boxes*), and *loxP* site (*solid triangle*) are indicated. (*D*) The mutant mice that carry the TCRγ-deficient (CγΔ) allele were intercrossed to produce TCRγ$^{+/+}$ (WT), TCRγ$^{+/-}$ (γ$^{+/-}$), and TCRγ$^{-/-}$ (γ$^{-/-}$) mice, and the corresponding WT and mutant alleles were typed by PCR analysis of tail DNA with each set of primers indicated. (*E*) γδ T cells are absent from the IEL compartment of γ$^{-/-}$ and αγ$^{-/-}$ mice. γ$^{-/-}$ Mice were crossed with α$^{-/-}$ mice to obtain WT (α$^{+/-}$ × γ$^{+/-}$), γ$^{-/-}$ (α$^{+/-}$ × γ$^{-/-}$), α$^{-/-}$ (α$^{-/-}$ × γ$^{+/-}$), and αγ$^{-/-}$ (α$^{-/-}$ × γ$^{-/-}$) littermate mice.

mation characterized by elongation of crypts was much milder in αγ$^{-/-}$ mice as compared with α$^{-/-}$ mice (Figure 3*A*). Although the body weight was comparable between αγ$^{-/-}$ and α$^{-/-}$ mice, it was evident that colonic weight was significantly decreased in αγ$^{-/-}$ mice as compared with α$^{-/-}$ mice (Figure 3*B*). The disease score characterized by the thickening of colonic mucosa with crypt elongation and inflammatory cell infiltration was also significantly lower in αγ$^{-/-}$ mice than that rated in α$^{-/-}$ mice (Figure 3*C*). Although approximately 20% of 20- to 60-week-old α$^{-/-}$ mice displayed anorectal prolapse (ARP), it was not discerned in any of age-matched αγ$^{-/-}$ mice (Figure 3*D*). Notably, no difference was observed in the age of onset of colitis and in the incidence of colitis (~80%) among 20- to 32-week-old αγ$^{-/-}$ and α$^{-/-}$ mice. In addition, in comparison with administration of PBS (as control), adoptive transfer of γδ T cells that were purified from α$^{-/-}$ mice did not increase the incidence of colitis in the recipient αγ$^{-/-}$ mice. However, the transfer of γδ T cells exacerbated the severity of colitis in the recipient αγ$^{-/-}$ mice. As shown in Figure 3*E*, more severe inflammatory cell infiltration was observed in the inflamed colon of the recipient αγ$^{-/-}$ mice with γδ T-cell transfer as compared with control αγ$^{-/-}$ mice. Therefore, it is possible that γδ T cells may be involved in the exacerbation, but not induction, of UC-like colitis.

Decrease in the Colonic Neutrophils and Monocytes in the Absence of γδ T Cells

The above results indicate that the spontaneous colitis in α$^{-/-}$ mice is ameliorated by the absence of γδ T cells in αγ$^{-/-}$ mice. With these findings in mind, flow cytometric analysis of colonic LP cells isolated from WT, γ$^{-/-}$, α$^{-/-}$, and αγ$^{-/-}$ littermate mice at approximately 28 weeks of age was performed, and the representative results of 5 independent experiments are presented in Figure 4*A*. In this experiment, WT, γ$^{-/-}$, α$^{-/-}$, and αγ$^{-/-}$ littermate mice yielded 5.1 × 10^5, 6.1

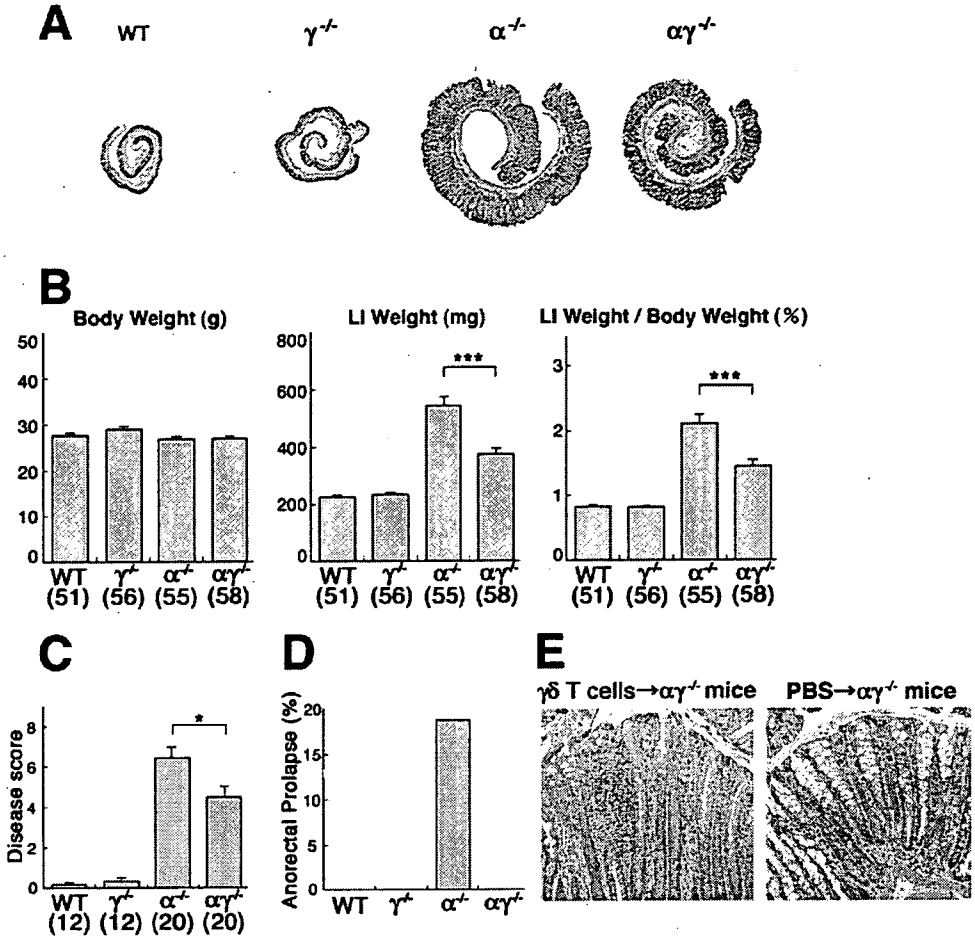

Figure 3. Colonic mucosal inflammation is milder in $\alpha\gamma^{-/-}$ mice lacking γδ T cells than in $\alpha^{-/-}$ mice possessing γδ T cells. (*A*) Representative histologic pictures of colon from WT, $\gamma^{-/-}$, $\alpha^{-/-}$, and $\alpha\gamma^{-/-}$ littermate mice. These mice were maintained in the same cages under specific pathogen-free conditions and examined at 28 weeks of age. (*B*) Body weight, wet weight of large intestine (LI weight), and ratio (%) of LI weight to body weight in WT, $\gamma^{-/-}$, $\alpha^{-/-}$, and $\alpha\gamma^{-/-}$ littermate mice at 20 to 32 weeks of age are shown. Values in parentheses are numbers of mice examined. $^{***}P < .001$. (*C*) Disease scores (0–10) of colitis in 24- to 32-week-old WT, $\gamma^{-/-}$, $\alpha^{-/-}$, and $\alpha\gamma^{-/-}$ mice were assessed. Values in parentheses are numbers of mice examined. $^{*}P < .05$. (*D*) Incidence of ARP in 24- to 60-week-old WT, $\gamma^{-/-}$, $\alpha^{-/-}$, and $\alpha\gamma^{-/-}$ mice. (*E*) The histologic findings (original magnification, ×20) of colon of recipient $\alpha\gamma^{-/-}$ mouse groups that received transfer of γδ T cells (*left panel*) and that received PBS (*right panel*).

× 10^5, 32.3 × 10^5, and 12.0 × 10^5 colonic LP cells, respectively. Based on the absolute numbers of infiltrated cells and the flow cytometry results shown in Figure 4*A*, it was evident that fewer Mac-1^+Ly-$6G^-$ cells and Mac-1^+Ly-$6G^+$ cells were present in the colonic LP cell population of $\alpha\gamma^{-/-}$ mice as compared with those of $\alpha^{-/-}$ mice. Monocytes express Mac-1 but not Ly-6G, whereas neutrophils express both Mac-1 and Ly-6G.[21] Therefore, our results suggest that, in addition to monocyte infiltration (Figure 4*A*), there is a marked infiltration of neutrophils in the inflamed colonic LP of $\alpha^{-/-}$ mice. We also confirmed our previous finding[15] that a remarkable increase in γδ T cells was observed in the inflamed colonic LP of $\alpha^{-/-}$ mice (Figure 4*A*).

Immunohistochemical examination of inflamed colons from $\alpha^{-/-}$ and $\alpha\gamma^{-/-}$ mice at approximately 28 weeks of age was performed to further confirm flow cytometric results. Consistent with the flow cytometric observations, significantly smaller numbers of Mac-1^+ cells and Ly-$6G^+$ cells were observed in the colonic LP of $\alpha\gamma^{-/-}$ mice as compared with those in the colonic LP of $\alpha^{-/-}$ mice (Figure 4*B*).

To investigate whether γδ T cells contribute to the generation of colonic environment for enhancing the migration of neutrophils and monocytes into the inflamed colon, we examined chemotactic activity of colonic extracts from $\alpha^{-/-}$ and $\alpha\gamma^{-/-}$ mice to neutrophils and monocytes (Figure 5*A*). As a result, chemotactic activity to neutrophils of colonic extracts from $\alpha\gamma^{-/-}$ mice was significantly weaker than that from $\alpha^{-/-}$ mice, whereas the chemotactic activities to monocytes of both extracts were almost comparable (Figure 5*B*). The marked infiltration of neutrophils into the inflamed colonic LP of $\alpha^{-/-}$ mice is most likely mediated by some factors, such as MIP-2 (Figure 5*A*), that are enhanced in the presence of γδ T cells.

Taking all of these results together, and in conjunction with our previous findings,[22] colonic γδ T cells of $\alpha^{-/-}$ mice exert aggravating effect on the UC-like colitis by increasing primarily the influx of neutrophils into the inflamed mucosa.

Attenuation of Colonic Proinflammatory Cascades by the Absence of γδ T Cells

In view of the severe colitis, increased infiltration of Mac-1^+Ly-$6G^+$ and Mac-1^+Ly-$6G^-$ cells, and marked production of neutrophil chemotactic factor(s) in the inflamed colonic LP of $\alpha^{-/-}$ mice, quantitative real-time

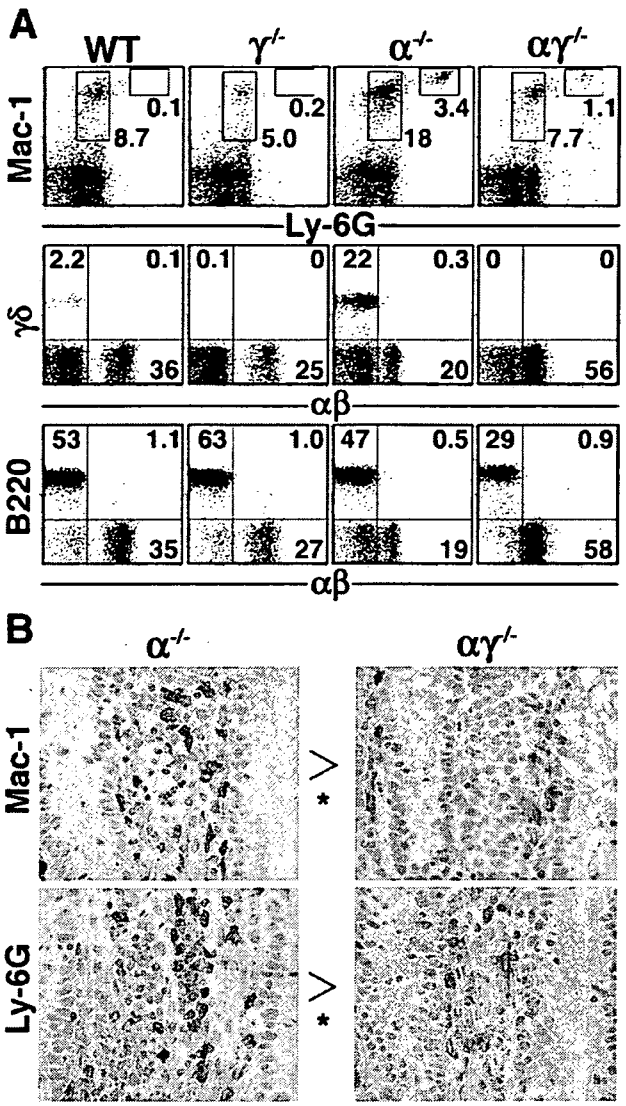

Figure 4. Decrease in colonic Mac-1$^+$Ly-6G$^-$ and Mac-1$^+$Ly-6G$^+$ cells in the absence of γδ T cells. WT (n = 3), $\gamma^{-/-}$ (n = 3), $\alpha^{-/-}$ (n = 4), and $\alpha\gamma^{-/-}$ (n = 4) mice from 28 weeks of age were examined. (*A*) Flow cytometric profiles of colonic LP cells. Absolute numbers of LP cells isolated from these WT, $\gamma^{-/-}$, $\alpha^{-/-}$, and $\alpha\gamma^{-/-}$ individuals were 5.1 × 10^5, 6.1 × 10^5, 32.3 × 10^5 and 12.0 × 10^5, respectively. (*B*) Representative immunohistochemical verification of the prominent infiltrations of Mac-1$^+$ and Ly-6G$^-$ cells into the inflamed colonic LP of $\alpha^{-/-}$ mice. Five tissue sections prepared from ascending colon to rectum per mouse, namely, 20 sections obtained from inflamed large intestines of $\alpha^{-/-}$ mice and those obtained from inflamed large intestines of $\alpha\gamma^{-/-}$ mice, were examined in a blinded fashion by 5 independent investigators, and the statistical difference in absolute numbers of Mac-1$^+$ and Ly-6G$^+$ cells between large intestinal mucosa from $\alpha^{-/-}$ and $\alpha\gamma^{-/-}$ mice were determined by 2-sided Mann–Whitney *U* test. *$P < .05$.

RT-PCR analysis and measurement of the amounts of representative proinflammatory cytokines as well as chemokines were performed to dissect further the role of γδ T cells in the UC-like colitis in $\alpha^{-/-}$ mice.

To this end, messenger RNA (mRNA) and proteins prepared from the large intestines of WT, $\gamma^{-/-}$, $\alpha^{-/-}$, and $\alpha\gamma^{-/-}$ mice were examined. Inflamed colonic tissues from $\alpha^{-/-}$ and $\alpha\gamma^{-/-}$ mice contained at least 10 times higher levels of cytokine (Table 1)- and chemokine (Table 2)-specific mRNA than those of WT and $\gamma^{-/-}$ mice except for IL-7 and IL-10 mRNA. In contrast to the mRNA from colonic tissues of $\alpha^{-/-}$ mice, those of $\alpha\gamma^{-/-}$ mice contained significantly smaller amounts of cytokine (TNF-α, IL-1β, IL-6, and TGF-β)- and chemokine (KC and MIP-2)-specific mRNA. With these observations in mind, we measured the amounts of representative cytokines as well as chemokines that had exhibited the differences in mRNA levels between the colonic tissues of $\alpha^{-/-}$ and $\alpha\gamma^{-/-}$ mice. First, in situ production of TNF-α, IL-1β, and IL-6 but not TGF-β proteins was significantly downregulated in the inflamed colonic mucosa of $\alpha\gamma^{-/-}$ mice as compared with that of $\alpha^{-/-}$ mice (Table 1). Second, KC and MIP-2 chemokines that are involved in the chemoattract of neutrophils and/or monocytes[23] were significantly decreased in large intestines of $\alpha\gamma^{-/-}$ mice compared with those in large intestines of $\alpha^{-/-}$ mice (Table 2).

To investigate the cell types responsible for the increases in these proinflammatory cytokines and chemokines, real-time RT-PCR analysis of mRNA present in the purified cell subsets from the inflamed colonic LP of $\alpha^{-/-}$ and $\alpha\gamma^{-/-}$ mice was performed (see Supplementary Figure 1 online at www.gastrojournal.org). The IL-1β and MIP-2 mRNA were expressed preferentially by Gr-1$^+$ cells, F4/80$^+$ cells, and CD11c$^+$ cells in the colon, whereas IL-6 mRNA was mainly expressed by Gr-1$^-$F4/80$^-$CD11c$^-$ cell populations. Expression levels of TNF-α- and KC-specific mRNA were comparable between all cell populations (Gr-1$^+$ cells, F4/80$^+$ cells, CD11c$^+$ cells, and Gr-1$^-$F4/80$^-$CD11c$^-$ cells) examined. Finally, the expression levels of these cytokine- and chemokine-specific mRNA in every cell subset were lower in cells from $\alpha\gamma^{-/-}$ mice than those in cells from $\alpha^{-/-}$ mice (see Supplementary Figure 1 online at www.gastrojournal.org).

Discussion

The $\alpha^{-/-}$ mice spontaneously develop colitis that shares many features with human UC.[16,24] Commensal enteric flora is required for the development of this colitis as indicated by the absence of colitis in $\alpha^{-/-}$ mice that are maintained under germ-free conditions.[22,25] The number of colonic γδ T cells drastically decreases in the $\alpha^{-/-}$ mice under germ-free conditions.[22] However, the study to identify the role of γδ T cells in the UC-like chronic colitis in $\alpha^{-/-}$ mice has been hampered by the difficulty in generating TCRαδ double mutant ($\alpha\delta^{-/-}$) mice because of the genomic organization of these TCR genes.[20] In the present study, we overcame this problem by newly generating $\gamma^{-/-}$ mice and subsequently crossing these mice with $\alpha^{-/-}$ mice to generate TCRα double mutant mice that lacked γδ T cells. By using these $\alpha\gamma^{-/-}$ mice, we herein provide a novel insight into the role of γδ T cells

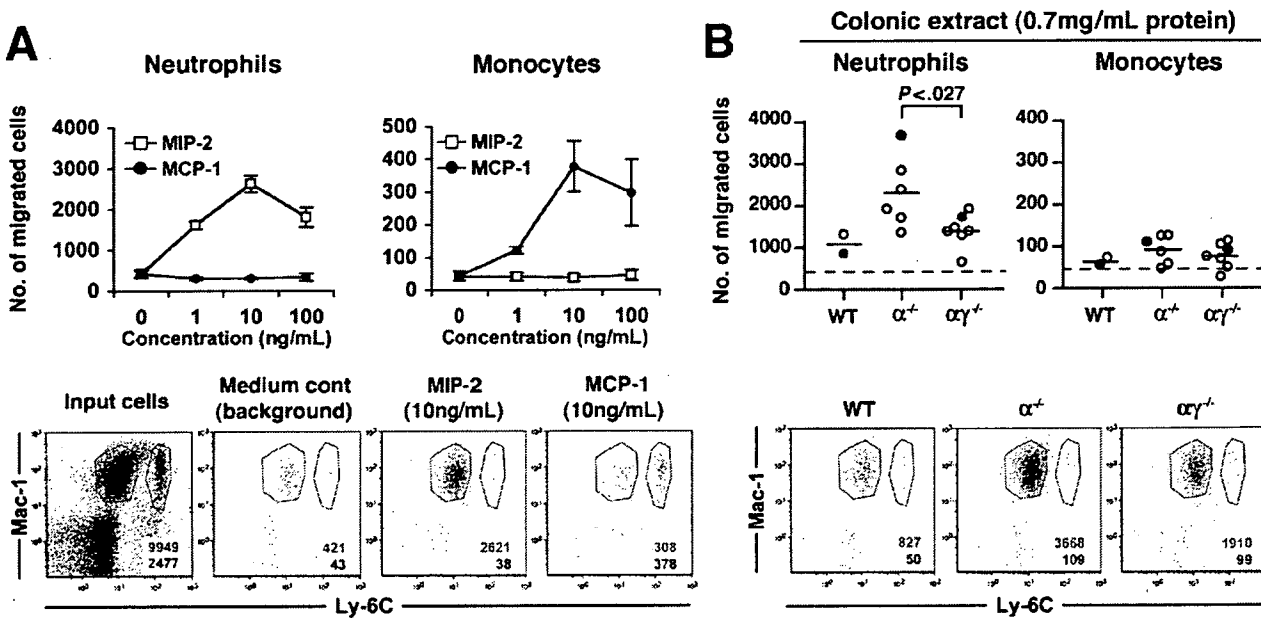

Figure 5. Chemotactic activity of colonic extracts from WT, $\alpha^{-/-}$, and $\alpha\gamma^{-/-}$ mice to neutrophils and monocytes. (*A*) The number of neutrophils and monocytes migrated in response to the increasing concentration of MIP-2 (*open square*) and MCP-1 (*solid circle*). The representative flow cytometric profiles are shown in the *lower panels*, and *red* and *blue gates* indicate the neutrophils and monocytes, respectively. *Colored numbers* represent means of the number of cells in each gate. (*B*) Chemotactic responses of neutophils and monocytes to colonic extracts (0.7 mg/mL protein) from WT, $\alpha^{-/-}$, and $\alpha\gamma^{-/-}$ mice, and each *circle* represents an individual mouse. *Horizontal bars* show mean values, and *dotted lines* indicate the number of migrated cells in medium alone. The representative flow cytomeric profiles of 3 individual animals indicated by the *solid red* and *blue circles* (*upper panels*) are shown in the *lower panels*, and *red* and *blue gates* indicate the neutrophils and monocytes, respectively.

that contributes to the exacerbation of UC-like colitis in $\alpha^{-/-}$ mice.

There is growing evidence supporting the fact that γδ T cells are part of the innate immune system and play an active multifaceted immunoregulatory role in the coordinated innate and acquired immune responses that maintain the integrity of many organs containing epithelia.[1,5,26,27] Nevertheless, the details of γδ T-cell functions are still not well understood as compared with those of αβ T cells. γδ T cells might play a defensive role against infections by various pathogenic microorganisms because exaggerated and severe infectious diseases occur in $\delta^{-/-}$ mice.[28-33] However, the same $\delta^{-/-}$ mice have also been demonstrated to display an increased host resistance to infection.[34,35] With regard to this, it is noteworthy that $V\gamma1^{+}$ γδ T cells are reported to eliminate the

Table 1. Real-Time RT-PCR Analysis and ELISA Assay of Cytokines in the Colonic Tissues

	Cytokine							
Mice (n)	TNF-α	IL-1β	IL-6	TGF-β	IFN-γ	IL-7	IL-10	IL-12
RT-PCR (copies per 10^3 HPRT)								
WT (5)	11.4 ± 0.53	6.86 ± 0.55	2.45 ± 0.64	123 ± 14.6	ND	11.7 ± 1.03	2.63 ± 0.28	0.82 ± 0.21
$\gamma^{-/-}$ (5)	9.20 ± 0.76	6.01 ± 0.61	2.14 ± 0.88	106 ± 10.7	ND	10.2 ± 0.78	2.09 ± 0.31	0.33 ± 0.09
$\alpha^{-/-}$ (7)	457 ± 35.7**	260 ± 18.6***	7.06 ± 1.04*	538 ± 48.6*	64.4 ± 8.90	11.0 ± 0.89	4.99 ± 0.72	9.58 ± 1.67
$\alpha\gamma^{-/-}$ (6)	205 ± 51.8**	98.5 ± 21.4***	2.93 ± 0.73*	319 ± 57.4*	45.0 ± 15.6	9.29 ± 1.11	6.42 ± 2.11	6.63 ± 1.01
ELISA (pg/mg protein)								
$\alpha^{-/-}$ (7)	100 ± 12.2**	975 ± 70.1**	8.24 ± 1.39**	2.09 ± 0.11	8.34 ± 1.50			
$\alpha\gamma^{-/-}$ (6)	27.0 ± 8.28**	647 ± 24.6**	2.92 ± 0.52**	2.57 ± 0.31	5.92 ± 2.56			

NOTE. All results are expressed as mean ± SE.
*$P < .05$.
**$P < .01$.
***$P < .001$.
ND, not detected

Table 2. Real-Time RT-PCR Analysis and ELISA Assay of Chemokines in the Colonic Tissues

	Chemokine					
Mice (n)	KC	MIP-2	GCP-2	MCP-1	MIP-1α	MIP-1β
RT-PCR (copies per 10^3 HPRT)						
WT (5)	6.05 ± 1.38	0.23 ± 0.01	12.3 ± 4.11	1.67 ± 0.17	0.78 ± 0.07	1.36 ± 0.22
$\gamma^{-/-}$ (5)	11.8 ± 1.19	0.22 ± 0.03	4.03 ± 1.49	1.77 ± 0.26	0.80 ± 0.04	1.42 ± 0.11
$\alpha^{-/-}$ (7)	382 ± 88.6*	101 ± 12.8**	721 ± 136	23.3 ± 4.37	35.0 ± 3.01	19.8 ± 0.88
$\alpha\gamma^{-/-}$ (6)	65.2 ± 17.4*	28.0 ± 9.80**	307 ± 168	16.0 ± 4.11	23.9 ± 7.34	14.2 ± 3.97
ELISA (pg/mg protein)						
$\alpha^{-/-}$ (7)	144 ± 22.4**	113 ± 21.2*	737 ± 139			
$\alpha\gamma^{-/-}$ (6)	32.4 ± 13.4**	44.9 ± 14.0*	414 ± 219			

NOTE. All results are expressed as mean ± SE.
*$P < .05$.
**$P < .01$.

macrophages infected with *Listeria monocytogenes*, whereas γδ T cells using Vγ elements other than Vγ1 gene appear to lack the ability to control macrophages but possess the ability to protect hosts from the infection-induced tissue injury.[36,37] In contrast to the beneficial function of γδ T cells by virtue of the fact that they can maintain the homeostasis of different types of organs,[1–5,8,27] a deleterious effect of γδ T cells on the regulation of neutrophil-mediated tissue damage after thermal (postburn) injury has been reported.[38] In various chronic and/or autoimmune inflammatory diseases, such as collagen-induced arthritis in mice[39] and murine insulin-dependent diabetes,[40] γδ T cells have been shown to exert a protective effect. Conversely, γδ T cells may directly contribute to autoimmune pathology of murine experimental allergic encephalomyelitis[41] as well as lupus in MRL/lpr mice.[42] Overall, both the beneficial and detrimental roles of γδ T cells in inflammatory process are evident.[43]

In chemically induced acute intestinal inflammation models (2,4,6-trinitrobenzene sulfonic acid- or dextran sulfate sodium-induced colitis), γδ T cells have been reported to play a protective role.[11–14] Depletion of γδ T cells by administration of anti-TCRγδ mAb into $TNF^{\Delta ARE}$ mice with a high frequency of spontaneous ileitis[44] did not lead to any histologic changes of ileitis.[45] However, transfer of bone marrow-derived γδ T cells has been shown to induce CD-like colitis in the bone marrow transplanted CD3εtg colitis model.[46] Although the role of γδ T cells in spontaneous chronic colitis remains to be explored to date, the results of the present study demonstrate the exacerbating effect of γδ T cells on the UC-like chronic colitis in $\alpha^{-/-}$ mice (Figures 3 and 4 and Tables 1 and 2). Interestingly, approximately 20% of $\alpha^{-/-}$ mice during 20 to 60 weeks of age suffered from ARP, whereas none of age-matched $\alpha\gamma^{-/-}$ mice showed ARP (Figure 3*D*). Of note, there were no differences in the age of onset of colitis and in the incidence of colitis (~80%) among 20- to 32-week-old $\alpha^{-/-}$ and $\alpha\gamma^{-/-}$ mice, but much more severe colitis was observed in $\alpha^{-/-}$ mice as compared with $\alpha\gamma^{-/-}$ mice. Therefore, it is possible that ARP may reflect increased severity of colitis and that γδ T cells may participate in the development of ARP.

Absence of γδ T cells in $\alpha\gamma^{-/-}$ mice leads to a significantly reduced production of TNF-α, IL-1β, and IL-6 proteins in the colonic tissues. These findings are consistent with our previous results[24] showing the involvement of TNF-α, IL-1β, and IL-6 in the perpetuation of inflammatory process in $\alpha^{-/-}$ mice. These inflammatory mediators have been shown to be important for host defense and wound repair.[47] Both KC and MIP-2 attract neutrophils to inflamed sites, and, in certain microbial infection, the collection of neutrophils leads to suppuration reflecting an active and vigorous host response against microbes. We also confirmed that colonic extracts from $\alpha\gamma^{-/-}$ mice exhibited the significantly weaker chemotactic activity to neutrophils than those from $\alpha^{-/-}$ mice. KC and MIP-2 mRNA expressions were lower in all purified cell subsets ($Gr\text{-}1^+$, $F4/80^+$, $CD11c^+$, and $Gr\text{-}1^-F4/80^-CD11c^-$ cells) from $\alpha\gamma^{-/-}$ mice than those from $\alpha^{-/-}$ mice. Therefore, in the presence of γδ T cells, many types of immune cells may be triggered to produce more chemokines, followed by infiltration of neutrophils into the colonic mucosa in $\alpha^{-/-}$ mice. γδ T-cell responsiveness that is manifested by recruitment and activation of inflammatory cells in which neutrophils predominate has also been reported.[1,31] In this context, it is of importance to note that the activity and severity of UC patients with increase in γδ T cells in the inflamed mucosa[9,10] (Figure 1) can be judged by the activation state of neutrophils in circulation[48] as well as by regional accumulation of neutrophils in the colonic crypt walls (cryptitis) or in the lumen of crypts (crypt abscess).[49]

The suppressive role of B cells[50] and the aggravating role of $TCR\beta^{dim}$ T cells[22,51] in the pathogenesis of colitis in $\alpha^{-/-}$ mice have been reported. Therefore, it is possible that γδ T cells may contribute to the exacerbation of this colitis by dampening regulatory B-cell function or by cooperating the colitogenic $TCR\beta^{dim}$ T cells. The possible complicated mechanism remains to be explored in the future. Levels of TNF-α and IL-1β mRNA in $F4/80^+$ cells

are higher in $\alpha^{-/-}$ mice compared with $\alpha\gamma^{-/-}$ mice (see Supplementary Figure 1 online at www.gastrojournal.org), suggesting that γδ T cells may activate macrophages to secrete large amounts of proinflammatory cytokines.

In conclusion, although γδ T cells at the inflamed colonic LP of $\alpha^{-/-}$ mice may protect intestinal epithelial injury, proinflammatory cytokines and neutrophil- and/or monocyte-chemoattractant chemokines induced by γδ T cells may directly and/or indirectly contribute to increased severity of UC-like chronic colitis in $\alpha^{-/-}$ mice. Further understanding of the molecular mechanisms of γδ T cell-mediated exacerbation of colitis in $\alpha^{-/-}$ mice will lead us to work out better therapeutic strategies for human UC.

Supplementary Data

Note: To access the supplementary material accompanying this article, visit the online version of *Gastroenterology* at www.gastrojournal.org, and at doi: 10.1053/j.gastro.2007.11.056.

References

1. Hayday A, Tigelaar R. Immunoregulation in the tissues by γδ T cells. Nat Rev Immunol 2003;13:233–242.
2. Jameson J, Ugarte K, Chen N, et al. A role for skin γδ T cells in wound repair. Science 2002;296:747–749.
3. Boismenu R, Havran WL. Modulation of epithelial cell growth by intraepithelial γδ T cells. Science 1994;266:1253–1255.
4. Komano H, Fijiura Y, Kawaguchi M, et al. Homeostatic regulation of intestinal epithelia by intraepithelial γδ T cells. Proc Natl Acad Sci USA 1995;92:6147–6151.
5. Mak TW, Ferrick DA. The γδ T-cell bridge: linking innate and acquired immunity. Nat Med 1998;4:764–765.
6. Podolsky DK. Inflammatory bowel disease. N Engl J Med 2002; 347:417–429.
7. Targan SR, Karp LC. Defects in mucosal immunity leading to ulcerative colitis. Immunol Rev 2005;206:296–305.
8. Shiohara T, Moriya N, Hayakawa J, et al. Resistance to cutaneous graft vs host disease is not induced in T-cell receptor δ gene-mutant mice. J Exp Med 1996;183:1483–1489.
9. McVay LD, Li B, Biancaniello R, et al. Changes in human mucosal γδ T cell repertoire and function associated with the disease process in inflammatory bowel disease. Mol Med 1997;3:183–203.
10. Yeung MM-W, Melgar S, Baranov V, et al. Characterization of mucosal lymphoid aggregates in ulcerative colitis: immune cell phenotype and TCR-γδ expression. Gut 2000;47:215–227.
11. Hoffmann JC, Peters K, Henschke S, et al. Role of T lymphocytes in rat 2,4,6-trinitrobenzene sulphonic acid (TNBS) induced colitis: increased mortality after γδ T cell depletion and no effect of αβ T cell depletion. Gut 2001;48:489–495.
12. Inagaki-Ohara K, Chinen T, Matsuzaki G, et al. Mucosal T cells bearing TCRγδ play a protective role in intestinal inflammation. J Immunol 2004;173:1390–1398.
13. Chen Y, Chou K, Fuchs E, et al. Protection of the intestinal mucosa by intraepithelial γδ T cells. Proc Natl Acad Sci U S A 2002;99:14338–14343.
14. Tsuchiya T, Fukuda S, Hamada H, et al. Role of γδ T cells in the inflammatory response of experimental colitis mice. J Immunol 2003;171:5507–5513.
15. Mizoguchi A, Mizoguchi E, Chiba C, et al. Cytokine imbalance and autoantibody production in T cell receptor-α mutant mice with inflammatory bowel disease. J Exp Med 1996;183:847–856.
16. Mombaerts P, Mizoguchi E, Grusby MJ, et al. Spontaneous development of inflammatory bowel disease in T cell receptor mutant mice. Cell 1993;75:274–282.
17. Hokama A, Mizoguchi E, Sugimoto K, et al. Induced reactivity of intestinal $CD4^+$ T cells with an epithelial cell lectin, galectin-4, contributes to exacerbation of intestinal inflammation. Immunity 2004;20:681–693.
18. de Bruijn MF, van Vianen W, Ploemacher RE, et al. Bone marrow cellular composition in *Listeria monocytogenes* infected mice detected using ER-MP12 and ER-MP20 antibodies: a flow cytometric alternative to different counting. J Immunol Methods 1998;217:27–39.
19. Itohara S, Mombaerts P, Lafaille J, et al. T cell receptor δ gene mutant mice: independent generation of αβ T cells and programmed rearrangements of γδ TCR genes. Cell 1993;72:337–348.
20. Davis MM, Bjorkman PJ. T-cell antigen receptor genes and T-cell recognition. Nature 1988;334:395–402.
21. Goren I, Kampfer H, Muller E, et al. Oncostatin M expression is functionally connected to neutrophils in the early inflammation phase of skin repair: implications for normal and diabetes-impaired wounds. J Invest Dermatol 2006;126:628–637.
22. Kawaguchi-Miyashita M, Shimada S, Kurosu H, et al. An accessory role of $TCR\gamma\delta^+$ cells in the exacerbation of inflammatory bowel disease in TCRα mutant mice. Eur J Immunol 2001;31: 980–988.
23. Charo IF, Ransohoff RM. The many roles of chemokines and chemokine receptors in inflammation. N Engl J Med 2006;354: 610–621.
24. Mizoguchi A, Mizoguchi E, Bhan AK. Immune networks in animal models of inflammatory bowel disease. Inflamm Bowel Dis 2003; 9:246–259.
25. Dianda L, Hanby AM, Wright NA, et al. T cell receptor-αβ-deficient mice fail to develop colitis in the absence of a microbial environment. Am J Pathol 1997;150:91–97.
26. Tonegawa S, Berns A, Bonneville M, et al. Diversity, development, and probable functions of γδ T cells. Cold Spring Harbor Symp Quant Biol 1989;54:31–44.
27. Havran WL. A role for epithelial γδ T cells in tissue repair. Immunol Res 2000;21:63–69.
28. Mombaerts P, Arnoldi J, Russ F, et al. Different roles of αβ and γδ T cells in immunity against an intracellular bacterial pathogen. Nature 1993;365:53–56.
29. Roberts SJ, Smith AL, Wet AB, et al. T-cell $\alpha\beta^+$ and $\gamma\delta^+$ deficient mice display abnormal but distinct phenotypes toward a natural, widespread infection of the intestinal epithelium. Proc Natl Acad Sci U S A 1996;93:11774–11779.
30. D'Souza CD, Cooper AM, Frank AA, et al. An anti-inflammatory role for γδ T lymphocytes in acquired immunity to *Mycobacterium tuberculosis*. J Immunol 1997;158:1217–1221.
31. King DP, Hyde DM, Jackson KA, et al. Cutting edge: protective response to pulmonary injury requires γδ lymphocytes. J Immunol 1999;162:5033–5036.
32. Moore TA, Moore BB, Newstead NW, et al. γδ-T cells are critical for survival and early proinflammatory cytokine gene expression during murine *Klebsiella* pneumonia. J Immunol 2000;165: 2643–2650.
33. Selin LK, Santolucito PA, Pinto AK, et al. Innate immunity to viruses: control of vaccinia virus infection by γδ T cells. J Immunol 2001;166:6784–6794.
34. Emoto M, Nishimura H, Sakai T, et al. Mice deficient in γδ T cells are resistant to lethal infection with *Salmonella choleraesuis*. Infect Immun 1995;63:3736–3738.

35. Uezu K, Kawakami K, Miyagi K, et al. Accumulation of γδ T cells in the lungs and their regulatory roles in Th1 response and host defense against pulmonary infection with *Cryptococcus neoformans*. J Immunol 2004;172:7629–7634.
36. Andrew EM, Newton DJ, Dalton JE, et al. Delineation of the function of a major γδ T cell subset during infection. J Immunol 2005;175:1741–1750.
37. Newton DJ, Andrew EM, Dalton JE, et al. Identification of novel γδ T-cell subsets following bacterial infection in the absence of $V\gamma1^+$ T cells: homeostatic control of γδ T-cell responses to pathogen infection by $V\gamma1^+$ T cells. Infect Immun 2006;74: 1097–1105.
38. Toth B, Alexander M, Daniel T, et al. The role of γδ T cells in the regulation of neutrophil-mediated tissue damage after thermal injury. J Leukoc Biol 2004;76:545–552.
39. Peterman GM, Spencer C, Sperling AI, et al. Role of γδ T cells in murine collagen-induced arthritis. J Immunol 1993;151:6546–6558.
40. Harrison LC, Dempsey-Collier M, Kramer DR, et al. Aerosol insulin induces regulatory CD8 γδ T cells that prevent murine insulin-dependent diabetes. J Exp Med 1996;184:2167–2174.
41. Rajan AJ, Gao Y-L, Raine CS, et al. A pathogenic role of γδ T cells in relapsing-remitting experimental allergic encephalomyelitis in the SJL mouse. J Immunol 1996;157:941–949.
42. Peng SL, Madaio MP, Highes DP, et al. Murine lupus in the absence of αβ T cells. J Immunol 1996;156:4041–4049.
43. Hayday A, Geng L. γδ cells regulate autoimmunity. Curr Opin Immunol 1997;9:884–889.
44. Kontoyiannis D, Pasparakis M, Piazzoro TT, et al. Impaired on/off regulation of TNF biosynthesis in mice lacking TNF AU-rich elements: implications for joint and gut-associated immunopathologies. Immunity 1999;10:387–398.
45. Kuhl AA, Loddenkemper C, Westermann J, et al. Role of γδ T cells in inflammatory bowel disease. Pathobiology 2002;70: 150–155.
46. Simpson SJ, Hollander GA, Mizoguchi E, et al. Expression of pro-inflammatory cytokines by $TCR\alpha\beta^+$ and $TCR\gamma\delta^+$ T cells in an experimental model of colitis. Eur J Immunol 1997;27: 17–25.
47. Nathan C. Points of control in inflammation. Nature 2002;420: 846–852.
48. Suematsu M, Suzuki M, Kitahora T, et al. Increased respiratory burst of leukocytes in inflammatory bowel diseases: the analysis of free radical generation by using chemiluminescence probe. J Clin Lab Immunol 1987;24:125–128.
49. Simmonds NJ, Allen RE, Stevens TR, et al. Chemiluminescence assay of mucosal reactive oxygen metabolites in inflammatory bowel disease. Gastroenterology 1992;103:186–196.
50. Sugimoto K, Ogawa A, Shimomura Y, et al. Inducible IL-12-producing B cells regulate Th2-mediated intestinal inflammation. Gastroenterology 2007;133:124–136.
51. Takahashi I, Kiyono H, Hamada S. $CD4^+$ T-cell population mediates development of inflammatory bowel disease in T-cell receptor α chain-deficient mice. Gastroenterology 1997;112:1876–1886.

Received April 11, 2007. Accepted November 15, 2007.

Address requests for reprints to: Hiromichi Ishikawa, MD, PhD, Department of Microbiology and Immunology, Keio University School of Medicine, 35 Shinanomachi, Shinjuku-ku, Tokyo 160-8582, Japan. e-mail: h-ishika@sc.itc.keio.ac.jp; fax: (81) 3-5360-1508.

Supported in part by a Grant-in-Aid for Creative Scientific Research, the Japan Society for the Promotion of Science (13GS0015); by Special Coordination Funds for Promoting Science and Technology from the Japanese Ministry of Education, Culture, Sports, Science, and Technology; and by Research on Specific Diseases, Japanese Ministry of Health, Labor, and Welfare (to H.I.); by Keio University Special Grant-in-Aid for Innovative Collaborative Research Projects (to T.H.); by National Institutes of Health grants DK47677 (to A.K.B.) and DK064351 (to A.M.); by the Center for the Study of Inflammatory Bowel Disease, Massachusetts General Hospital; and by 21st Century Center-of-Excellence (COE) Program for Life Science from MEXT (to M.S.).

The authors thank Dr Daniel K. Podolsky for his many valuable discussions and comments, Dr Leo Lefrancois for his critical reading of the manuscript, and Dr Atsuhiro Ogawa for his excellent technical assistance.

M.N. and Y.K. contributed equally to this work.

Y.K.'s current location is Department of Immunology, Kinki University School of Medicine, Osaka, Japan.

H.Y.'s current location is Health Research Foundation, Kyoto, Japan.

Conflicts of interest: No conflicts of interest exist.

T.N. was a research fellow supported by 21st Century COE Program for Life Science from MEXT and is now supported by Global COE Program for Human Metabolomic Systems Biology from MEXT (to M.S.).

GASTROENTEROLOGY 2007;133:559–573

Lamina Propria c-kit$^+$ Immune Precursors Reside in Human Adult Intestine and Differentiate Into Natural Killer Cells

HIROSHI CHINEN,[*,‡] KATSUYOSHI MATSUOKA,[*] TOSHIRO SATO,[*] NOBUHIKO KAMADA,[*] SUSUMU OKAMOTO,[*] TADAKAZU HISAMATSU,[*] TAKU KOBAYASHI,[*] HIROTOSHI HASEGAWA,[§] AKIRA SUGITA,[¶] FUKUNORI KINJO,[‡] JIRO FUJITA,[‡] and TOSHIFUMI HIBI[*]

[*]Division of Gastroenterology and Hepatology, Department of Internal Medicine, School of Medicine, Keio University, Tokyo, Japan; [‡]Department of Medicine and Therapeutics, Control and Prevention of Infectious Diseases, Graduate School of Medicine, University of the Ryukyus, Okinawa, Japan; [§]Department of Surgery, School of Medicine, Keio University, Tokyo, Japan; and [¶]Department of Surgery, Yokohama Municipal Citizen's Hospital, Yokohama, Japan

Background & Aims: **Recent studies have revealed that murine intestinal mucosa contains several kinds of lineage markers (lin)$^-$ c-kit$^+$ immune precursor cells. However, immune precursors in the human adult intestine have not been studied extensively.** ***Methods:*** **Lamina propria mononuclear cells and intraepithelial lymphocytes from surgically resected human adult intestine were examined for the surface antigen expression and cytokine profile by immunohistochemistry and flow cytometry. The transcriptional profile of these cells was analyzed by reverse-transcription polymerase chain reaction. The phenotypic and functional characterization of the in vitro differentiating cells from the precursors was examined by flow cytometry.** ***Results:*** **We identified lin$^-$ c-kit$^+$ cells scattered throughout lamina propria of the human adult intestine. These intestinal immune precursors expressed CD34, CD38, CD33, interleukin-2Rα, and interleukin-7Rα, and they had much more abundant expression of Id2, PU.1, SpiB1, and lymphotoxin than thymocytes. The lin$^-$ c-kit$^+$ immune precursors mainly differentiated into CD56$^+$ c-kit^{dim} cells during in vitro culture. These in vitro differentiating cells corresponded to intestinal natural killer (NK) cells, which had distinct characteristics from their peripheral counterparts, such as CD83 and integrin α_E expression, less cytotoxic activity, and higher interferon-γ production. Furthermore, both c-kit^{dim} cells and NK cells were increased in lamina propria of Crohn's disease, although there was no change for peripheral blood NK cells.** ***Conclusions:*** **The human intestine may have the unique NK cell differentiation system, which may contribute to maintenance of immune homeostasis in the intestine.**

The cellular components of the immune system, such as T cells, B cells, monocytes, granulocytes, macrophages, dendritic cells, and natural killer (NK) cells, are derived from common hematopoietic stem cells (HSCs) in the bone marrow. As a first step, HSCs differentiate into 2 distinct subsets: common myeloid progenitors and common lymphoid progenitors. Although common myeloid progenitors ultimately differentiate into myeloid cells such as monocytes, granulocytes, macrophages, and dendritic cells,[1] common lymphoid progenitors differentiate into B-cell precursors and common T- and NK-cell precursors (T/NKPs).[2] T/NKPs subsequently differentiate into NKPs and T-cell precursors.[3–5] These steps are assumed to proceed mainly in the bone marrow, which is regarded as the most important site for primary immune cell differentiation.

A unique immune system has developed in the intestine. The intestinal immune system includes Peyer's patches, isolated lymphoid follicles, mesenteric lymph nodes (MLN), lamina propria mononuclear cells (LPMCs), and intraepithelial lymphocytes (IELs). This intestinal immune system maintains immunologic homeostasis against gut luminal antigens. In addition to these components, the intestine has become recognized as a site for differentiation of immune cells. Recent studies have revealed that murine intestinal mucosa contains immune precursor cells, which are lymphoid tissue inducer cells (LTi)[6,7] in the fetus and cryptopatch (CP) cells[8] in the adult. Both LTi and CP cells express c-kit, IL-7 receptor α subunit (IL-7Rα), IL-2Rα, CD44, and CD4^{dim}. These surface phenotypes are similar to those of common lymphoid progenitors in bone marrow, and LTi and CP cells have been reported to develop in situ into Peyer's patches[6,7,9] and extrathymic T cells of IELs,[10,11] respectively. In addition, a recent study suggested that CP cells can function as adult LTi by developing into isolated lymphoid folli-

Abbreviations used in this paper: CP, cryptopatch; HSC, common hematopoietic stem cell; IENK, intraepithelial natural killer cell; IFN, interferon; IL, interleukin; IL-7Rα, IL-7 receptor α subunit; Lin, lineage markers; LPMCs, lamina propria mononuclear cells; LPNKs, lamina propria natural killer cells; LTi, lymphoid tissue inducer cells; MLN, mesenteric lymph nodes; NK, natural killer; PBL, peripheral blood lymphocytes; PBNKs, peripheral blood natural killer cells; PCR, polymerase chain reaction; pTα, pre-T cell receptor chain α; RAG, recombination activating gene; SEM, standard error of the mean; T/NKPs, common T and natural killer cell precursors; TNF, tumor necrosis factor.

0016-5085/07/$32.00
doi:10.1053/j.gastro.2007.05.017

cles rather than IELs in normal adult mice.[12] The immune precursor cells in the murine intestine have been investigated extensively; however, only a few reports have referred to immune precursor cells in the human intestine. A recent study showed that $CD3^-$ $CD7^+$ cells in the human fetal intestine express messenger RNA (mRNA) for pre-T-cell receptor chain α (pTα), which is essential for early T-cell differentiation.[13] It also shows that these cells can give rise to $CD3^+$ T cells in vitro and in vivo, using severe combined immunodeficient (SCID) mice engrafted with human fetal intestine.[14] It also has been reported that recombination activating gene (RAG)-1 and RAG-2 mRNA can be detected in the intestinal mucosa of human infants.[15,16] Moreover, $CD3^-$ $CD2^+$ $CD7^+$ cells in the human adult jejunum have been shown to express RAG mRNA as well as pTα mRNA.[16] All these reports have examined intestinal immune precursors in light of extrathymic T-cell differentiation. However, considering the reports on the murine intestine, we assume that more immature immune precursor cells, such as LTi, also may reside in the human adult intestine.

To verify this hypothesis, we first analyzed human adult intestine immunohistochemically, focusing on expression of c-kit, which is a receptor for stem cell factor and is known to be expressed on immune precursor cells such as HSCs.[17] Although intensive analysis did not reveal any $c\text{-}kit^+$ cell clusters such as CP, we found a considerable number of $c\text{-}kit^+$ cells scattered in the lamina propria. We next characterized with flow cytometry these $c\text{-}kit^+$ cells in LPMCs isolated from human adult intestine, which revealed that the $c\text{-}kit^+$ cells in the intestine have phenotypes identical to T/NKPs in the fetal liver[18] and thymus.[19] The $c\text{-}kit^+$ cells mainly were committed to the NK cell lineage in vitro. We also found unique characteristics of mature NK cells residing in the human adult intestine. These results suggest that $c\text{-}kit^+$ cells should differentiate into intestinal NK cells. Furthermore, NK cell differentiation is accelerated in Crohn's disease (CD), indicating that this intestinal NK cell differentiation system may play a role in the pathogenesis of chronic intestinal inflammation. Thus, we were able to show differentiation of intestinal NK cells from $c\text{-}kit^+$ cells in the human adult intestine, which may contribute to maintenance of intestinal immune homeostasis.

Materials and Methods

Tissue Samples

Normal intestinal mucosa and MLN were obtained from macroscopically and microscopically unaffected areas of patients with colon cancer. Intestinal mucosa also was obtained from surgically resected specimens from patients with CD or ulcerative colitis (UC), diagnosed on the basis of clinical, radiographic, endoscopic, and histologic findings, according to established criteria.[20,21] In all samples from patients with CD or UC, the degree of inflammation was histologically moderate to severe. All experiments were approved by the institutional review board and written informed consent was obtained from all the patients.

Histologic Analysis

Tissue sections were treated according to well-established methods. Intestinal specimens were fixed with 4% paraformaldehyde (Wako Pure Chemical Industries, Osaka, Japan) and embedded in paraffin. Sections from paraffin-embedded blocks were deparaffinized and stained with H&E (Sakura Finetech Japan, Tokyo, Japan). For immunohistochemical staining, deparaffinized sections were heated at 100°C for 20 minutes in 10 mmol/L sodium citrate buffer (pH 6.0) in a microwave oven. For the enzyme-labeled antibody method, each section was treated with 3% H_2O_2 (Wako) in 100% methanol and then incubated with normal rabbit serum (Nichirei Biosciences, Tokyo, Japan) for 15 minutes at room temperature to block nonspecific reactions. Thereafter, sections were treated with rabbit anti-human c-kit Ab (Dako Cytommation, Glostrup, Denmark) and incubated at 4°C overnight. Primary antibodies were washed out and sections were incubated with Histofine anti-rabbit Simplestain Max-PO (Nichirei), and visualized with 3-3'-diaaminobenzidine (Nichirei) for peroxidase and counterstained with hematoxylin. Sections incubated with the IgG fraction of normal rabbit serum (Dako) served as negative controls. For identification of mast cells, deparaffinized sections were stained with .05% toluidine blue solution, pH 4.1 (Wako). Mast cells were stained red-purple and other cells were stained blue.

Preparation of LPMCs, IELs, Peripheral Blood Lymphocytes (PBLs), and MLN Cells

LPMCs and IELs were isolated from intestinal specimens using modifications of previously described techniques.[22,23] Briefly, dissected mucosa was incubated in calcium and magnesium-free Hanks' balanced salt solution (Sigma-Aldrich, St. Louis, MO) containing 2.5% heat-inactivated fetal bovine serum (BioSource, Camarillo, CA) and 1 mmol/L dithiothreitol (Sigma-Aldrich) to remove mucus. The mucosa then was incubated in Hanks' balanced salt solution containing 1 mmol/L ethylenediaminetetraacetic acid (EDTA) (Sigma-Aldrich) for 60 minutes at 37°C. During this treatment, IELs and epithelial cells were removed from the tissue. Tissues were collected and incubated in Hanks' balanced salt solution containing .02% collagenase type 3 (Worthington Biochemical, Freehold, NJ) for 60 minutes at 37°C. The fraction was pelleted and resuspended in 40% Percoll solution (Amersham Biosciences, Piscataway, NJ), then layered on 60% Percoll before centrifugation at 2000 rpm for 20 minutes at room temperature. Viable LPMCs were recovered from the 40%–60% layer interface. For isolation of IELs, after EDTA treatment the supernatants were

collected and filtered through a glass-wool column to deplete cell debris and sticky cells. Cells were centrifuged over a 40%–60% Percoll solution density gradient. IELs were recovered from the layer interface. PBLs were isolated from heparinized peripheral blood samples by density gradient centrifugation using Lymphoprep (Nycomed Pharma, Oslo, Norway). For isolation of MLN cells, MLN were squeezed and passed through sterile nylon mesh to create single-lymphocyte suspensions.[24]

Giemsa Stain

The lin$^-$ c-kit$^+$ cells and the mast cells in LPMCs were sorted by Epics Altra with the HyPerSort cell sorting system (Beckman-Coulter, Fullerton, CA). The purity of the sorted cells was greater than 98% by postsorting analysis. After spreading the sorted cells on glass slides they were air dried, then the cells were fixed with methanol and stained with pH 6.4 Giemsa solution (Merck, Whitehouse Station, NJ), and they were observed by light microscope.

Flow Cytometric Analysis of c-kit$^+$ LPMCs Differentiation Markers

Cell surface fluorescence intensity was assessed using a FACSCalibur analyzer and analyzed with Cell Quest software (BD Biosciences, San Jose, CA). Dead cells were excluded with propidium iodide staining. The lineage marker monoclonal antibodies that were used were the available Lineage Cocktail 1 (BD Biosciences). Lineage Cocktail 1 included CD3 (SK7), CD14 (MϕP9), CD16 (3G8), CD19 (SJ25C1), CD20 (L27), and CD56 (NCAM16.2). All the antibodies were purchased from BD Biosciences except for CD2, CD20, CD56 (MEM188), and NKG2D, which were purchased from eBiosciences (San Diego, CA); CCR7, CXCR5, and IL-18Rα were purchased from R&D systems (Minneapolis, MN); CD133 was purchased from Miltenyi Biotec (Bergisch, Gladbach, Germany); and CX3CR1 was purchased from Medical & Biological Laboratories (Nagoya, Japan).

Quantitative Real-Time, Reverse-Transcription Polymerase Chain Reaction Analysis

Cells were sorted by Epics Altra with the HyPerSort cell sorting system (Beckman-Coulter). The purity of the sorted cells was always greater than 98% by postsorting analysis. Total RNA was extracted using the RNeasy Micro Kit (Qiagen, Hilden, Germany), and total thymocyte RNA was purchased from BD Biosciences. Total RNA was treated with Qiagen DNase I to remove any contaminating genomic DNA. Absence of amplification of contaminating genomic DNA was ascertained by polymerase chain reaction (PCR) in which RNA was used as a template. Complementary DNA was synthesized using the Superscript first-strand synthesis system for reverse-transcription PCR (Invitrogen, Carlsbad, CA), according to the manufacturer's instructions. Semiquantitative real-time, reverse-transcription PCR was performed using TaqMan universal PCR master mix (Applied Biosystems, Foster City, CA) and on-demand gene-specific primers. The fluorogenic probes were as follows: RAG-1, RAG-2, preTCRα, Id2, PU.1, SpiB1, lymphotoxin α, lymphotoxin β, and β-actin, which all were purchased from Applied Biosystems. Cycling conditions for PCR amplification were 95°C for 10 minutes, followed by 45 cycles of 94°C for 15 seconds, and 60°C for 1 minute. Transcription of mRNA was assessed on a DNA Engine Opticon 2 System and analyzed with Opticon monitor software (MJ Research, Waltham, MA). All samples were analyzed in triplicate.

Lin$^-$ c-kit$^+$ LPMCs In Vitro Culture

CD3$^+$ and CD56$^+$ cells were removed from LPMCs using a magnetic cell-sorting system (MACS; Miltenyi Biotec) according to the manufacturer's instructions. The CD3$^-$ CD56$^-$ LPMCs were cultured at a concentration of 1×10^6/mL in complete medium consisting of 1640 RPMI (Sigma-Aldrich) supplemented with GlutaMAX (Invitrogen), 10% heat-inactivated fetal bovine serum (BioSource), 10 mmol/L HEPES (Invitrogen), 50 μmol/L 2-mercaptoethanol (Wako), 100 U/mL penicillin, and 100 mg/mL streptomycin (Invitrogen). The cultures were maintained in a humidified atmosphere at 37°C in 5% CO_2 for 72 hours. All samples were cultured in duplicate.

Isolation of Peripheral Blood NK Cells and Lamina Propria NK Cells

CD56^{dim} (CD3$^-$ CD14$^-$ CD16$^+$ CD56$^+$) peripheral blood NK (PBNK) cells and CD56^{bright} (CD3$^-$ CD14$^-$ CD16$^-$ CD56$^+$) PBNKs were isolated from PBLs by using MACS (Miltenyi Biotec) according to the manufacturer's instructions. Lamina propria NK (LPNK) cells (CD3$^-$ CD14$^-$ CD56$^+$) also were isolated with MACS. The percentage of each isolated NK cell was evaluated by flow cytometry and routinely was greater than 95%.

Cytotoxicity Assay

The cytotoxicity of NK cell subsets against the NK-sensitive K562, a human erythroleukemic cell line (American Type Culture Collection, Rockville, MD), was measured by using a previously described protocol[25] with minor modifications.

NK Cell Cytokine Production

A total of 1×10^6 cells in 1 mL complete RPMI 1640 medium (Sigma-Aldrich) were stimulated with 10 ng/mL IL-12 (Medical & Biological Laboratories) and 100 ng/mL IL-15 (R&D) or 10 ng/mL IL-12 (Medical & Biological Laboratories) and 100 ng/mL IL-18 (Medical & Biological Laboratories) for 8 hours at 37°C. After stimulation, interferon-γ (IFN-γ) or tumor necrosis factor-α

(TNF-α) production were detected using the Cytokine Secretion Assay Cell Detection Kit (Miltenyi Biotec) according to the manufacturer's instructions, defining cells with antibodies against CD3, CD56, or CD117 (BD Biosciences) and propidium iodide. IFN-γ and TNF-α in cell culture supernatant also were measured using human Th1/Th2 cytokine beads array kit (BD Biosciences) according to the manufacturer's protocol.

Transplantation of the Human lin⁻ c-kit⁺ LPMCs Into RAG-2⁻/⁻ Mice

C57BL/6J background RAG-2$^{-/-}$ mice (Central Institute for Experimental Animals, Kanagawa, Japan) were housed under specific pathogen-free conditions at the animal center of Keio University (Tokyo, Japan). All experiments using mice were approved by and performed according to the guidelines of the animal committee of Keio University. The human lin⁻ c-kit⁺ LPMCs cells (1.3–1.5 × 10^5) were injected intraperitoneally into 8-week-old RAG-2$^{-/-}$ mice. LPMCs, IELs, and splenic lymphocytes were isolated and examined for human lineage markers and human CD117 monoclonal antibody (BD Biosciences) by flow cytometry. For in vitro differentiation, isolated LPMCs were cultured with complete medium in the presence of 100 U/mL human recombinant IL-2 (eBiosciences) or 100 ng/mL IL-15 (R&D) for 7 days. Cultured cells were stained by human CD3 and CD56 monoclonal antibody (BD Biosciences) and assessed by flow cytometry. All samples were cultured in duplicate.

Statistical Analysis

Statistical analysis was performed by using STATVIEW software version J-5.0 (Abacus Concepts, Berkeley, CA), StatMate III software version 3.05 (ATMS, Tokyo, Japan), and GraphPad Prism software version 4.0 (GraphPad Software Inc., San Diego, CA). Differences at a P value of less than .05 were considered significant. All data are expressed as means ± standard error of the mean (SEM).

Results

Presence of Non–Cluster-Forming Lineage Markers (lin)⁻ c-kit⁺ Lymphocytes in the Human Adult Intestine

We first tried to identify c-kit⁺ cells in the human adult intestine by immunohistochemistry. We could not find any c-kit⁺ cell clusters such as murine CP cells; however, we found a considerable number of c-kit⁺ cells scattered in the intraepithelial space, lamina propria, and submucosal layers of both the ileum and colon (Figure 1*A* and *B*). The c-kit expression on IELs was dimmer than that on LPMCs (Figure 1*B* and *I*). Furthermore, the c-kit⁺ IELs were found only in the intraepithelial space of crypts, but not in that of villi (data not shown). Because c-kit also is expressed on mast cells,[26] sequential sections were stained metachromatically with toluidine blue, which is useful for identifying mast cells (Figure 1*C*). Although most of the c-kit⁺ cells in the submucosal layer and a part of the c-kit⁺ cells in the lamina propria presented metachromasia (Figure 1*G* and *H*), a considerable proportion of the c-kit⁺ LPMCs and IELs did not (Figure 1*E*, *F*, *I*, and *J*). We next analyzed with flow cytometry LPMCs isolated from human adult intestine. Mast cells were excluded by taking advantage of their complex granular morphology and higher c-kit expression[27] (Figure 2*A*). The other c-kit⁺ population, distinct from mast cells, was consistent with a typical lymphoid cell gate in forward- and side-scatter diagrams and was used for further analysis. We then examined these c-kit⁺ cells for lineage markers as follows: CD3, CD14, CD16, CD19, CD20, and CD56. The blot diagram clearly identified 2 distinct c-kit⁺ populations: lin⁻ c-kit⁺ and lin⁻ c-kit^{dim} cells (Figure 2*B*). The lin⁻ c-kit⁺ subset occupied 1.97% ± .15%, whereas the lin⁺ c-kit^{dim} subset occupied 1.29% ± .22% of the total LPMCs (n = 10). The lin⁻ c-kit⁺ cells were different from mast cells morphologically, and they seemed to be small immature lymphoid cells about 7 μm in diameter (Figure 2*C*). A similar number of lin⁻ c-kit⁺ cells were detected in LPMCs from both the ileum and colon; however, they barely were recognized in IELs, MLN cells, or PBLs (Figure 2*B*). In contrast, the lin⁺ c-kit^{dim} subset also was present in IELs, which was consistent with the immunohistochemical finding that c-kit expression on IELs was dimmer than that on LPMCs (Figure 1*B* and *I*). We assumed that these lin⁻ c-kit⁺ cells were immune precursor cells in the intestine.

Characterization of the lin⁻ c-kit⁺ and lin⁺ c-kit^{dim} Subsets

To characterize further the 2 c-kit⁺ populations in LPMCs, we examined the expression of various surface stem cell markers. The lin⁻ c-kit⁺ cells also expressed CD34 (Figure 3*A*), which is another marker for HSCs.[28] However, CD34 expression on lin⁻ c-kit⁺ cells was lower than that on HSCs (Figure 3*A*). It is reported that the expression of CD34 decreases during differentiation, therefore, lower CD34 expression may reflect a later stage in the hematopoietic lineage.[29] The lin⁻ c-kit⁺ cells in LPMCs expressed CD38^{dim}, Thy-1, and CD45RA (Figure 3*A*), which corresponds to the phenotype of T/NKPs in fetal liver[18] and thymus.[19] Furthermore, they expressed IL-7Rα, IL-2Rα, CD44, CCR7, and CXCR5 (Figure 3*B*), which are expressed on immune precursor cells such as mouse LTi and CP cells. Importantly, a small number of the lin⁻ c-kit⁺ cells in LPMCs expressed IL-2Rβ and CD161, which are known as NK cell markers (Figure 3*B*). The lin⁻ c-kit⁺ cells were negative for CD56 when examined with clone NCAM 16.2 and MEM 188; however, a small fraction of the cells were weakly positive for clone B159. It is interesting to note that this subset expressed CD33, a known marker of myeloid lineage cells (Figure 3*A* and *B*).[30]

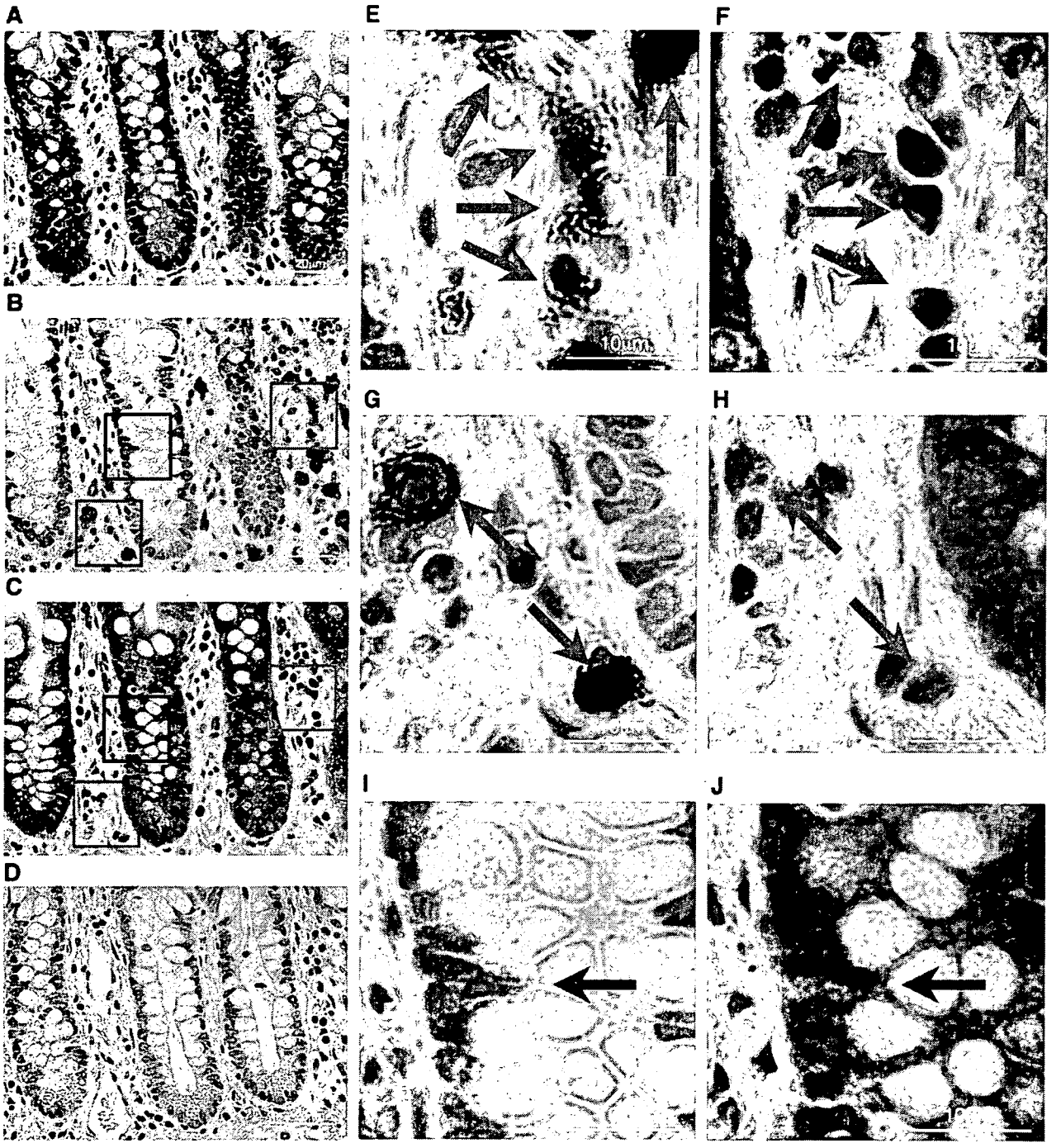

Figure 1. Identification of c-kit–expressing cells in the human adult intestine. Sequential sections of ileal mucosa were stained with (*A*) H&E, (*B*) c-kit antibody by 3-3′-diaaminobenzidine–enhanced immunoperoxidase and counterstained with hematoxylin, (*C*) toluidine *blue* to identify mast cells, and (*D*) negative control. The high-power image of representative c-kit$^+$ cells (*G*, *H*) with metachromatic staining (*red frame*) or (*E*, *F*) without metachromatic staining (*blue frame*) metachromatic staining. The high-power image of a (*I*) representative c-kit$^+$ IEL without metachromatic staining is shown in the (*J*) *black frame*.

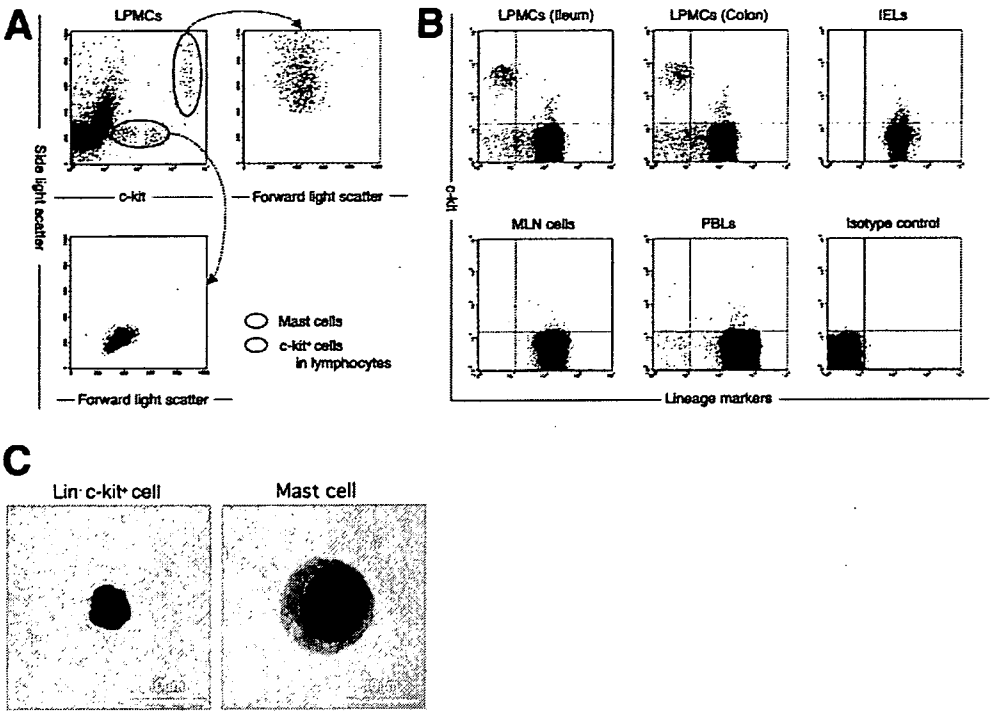

Figure 2. Flow cytometry of lin$^-$ c-kit$^+$ subset of LPMCs isolated from human adult intestine. (*A*) LPMCs were highlighted with c-kit expression and side-light scatter blotting (*upper left*). Side-light scatter high and c-kit high cells (red oval), which represented mast cells, were expanded further with side- and forward-side–scatter blotting (*upper right*). The cells with lower c-kit expression and lower side light scatter (*blue oval*) were expanded with the side- and forward-side–scatter blotting (*bottom left*). These cells were within a typical lymphoid cell gate. (*B*) LPMCs from ileum or colon, IELs, PBLs, and MLN cells in the lymphoid gate were analyzed for expression of c-kit and lineage markers (CD3, CD14, CD16, CD19, CD20, and CD56). The data shown are representative of 6 independent experiments. (*C*) The lin$^-$ c-kit$^+$ cells and the mast cells from LPMCs were stained with Giemsa solution.

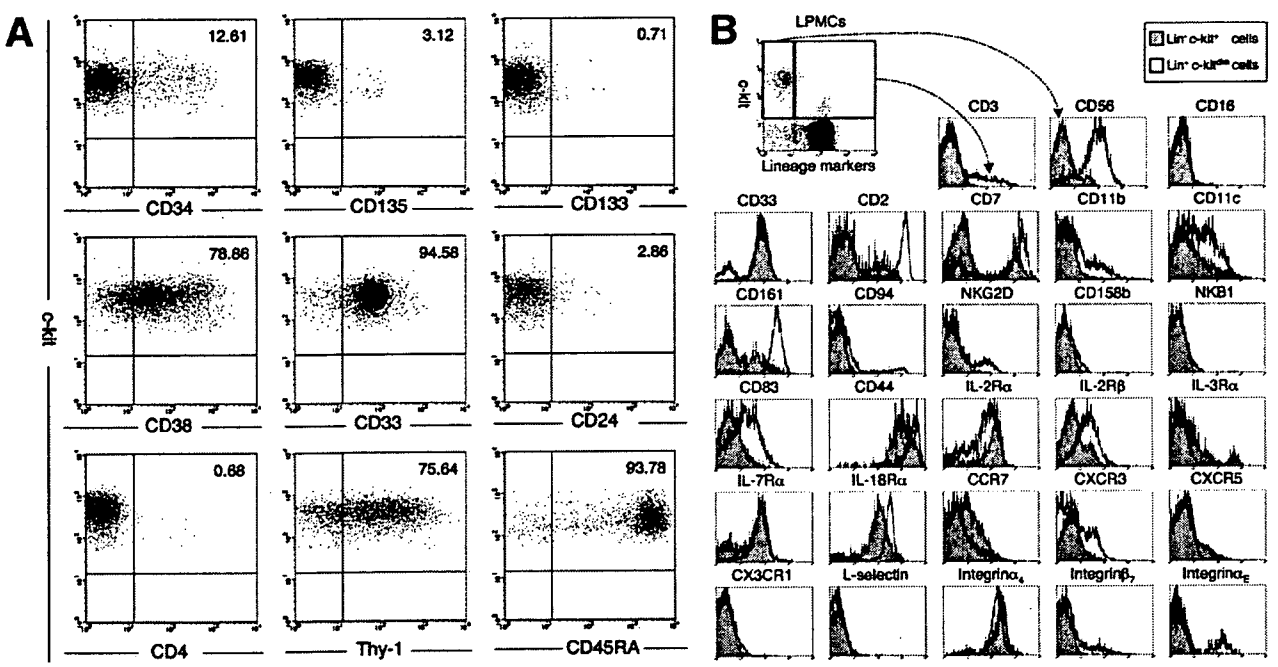

Figure 3. Characterization of the lin$^-$ c-kit$^+$ and lin$^+$ c-kit^{dim} subsets of LPMCs. (*A*) Stem cell marker expression was analyzed in the lin$^-$ c-kit$^+$ subset of LPMCs. (*B*) The lin$^-$ c-kit$^-$ subset (*gray histograms*) and the lin$^+$ c-kit^{dim} subset (*black lines*) of LPMCs were analyzed for the expression of several cell surface antigens. The data shown are representative of at least 5 experiments for each surface marker.

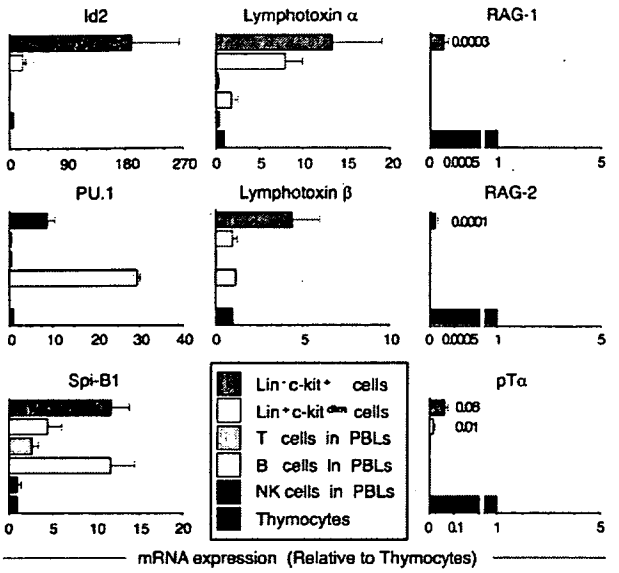

Figure 4. The lin⁻ c-kit⁺ subset has abundant mRNA for Id2, PU.1, SpiB1, and lymphotoxin α and β mRNA transcripts for each gene were quantified using real-time reverse-transcription PCR. In each sample, mRNA transcripts were normalized to those of β-actin. The expression value of each mRNA is shown as a ratio against that of thymocytes. Peripheral T, B, and NK cells were used as controls. Results are expressed as means ± SEM. The data are representative of 4 samples.

We next analyzed the lin⁺ c-kit^{dim} subset in LPMCs (Figure 3*B*). The lin⁺ c-kit^{dim} cells expressed only CD3 and CD56 among the lineage markers, and CD56⁺ cells predominated over CD3⁺ cells. The lin⁺ c-kit^{dim} subset also expressed other NK markers, IL-2Rβ and CD161, and these phenotypes corresponded to those of NKPs.[31,32] Interestingly, they expressed CD83 (Figure 3*B*), but they did not express other dendritic cell markers such as CD80, CD86, and CD209 (data not shown). It was also an intriguing finding that a fraction of these cells expressed integrin α_E, known as an IEL marker (Figure 3*B*).[33]

With the surface antigen expression patterns, the lin⁻ c-kit⁺ cells in the LPMCs were reminiscent of T/NKPs. On the other hand, the lin⁺ c-kit^{dim} subset likely may be a group of cells that already have begun differentiation into NK cells.

The lin⁻ c-kit⁺ Subset Has Abundant mRNA for Id2, PU.1, SpiB1, and Lymphotoxin

To confirm further the immature nature and differentiation potential of the lin⁻ c-kit⁺ cells, we examined the mRNA expression of several transcription factors essential for HSC differentiation. PU.1 and SpiB1 play important roles in HSC differentiation[34,35] and Id2 is essential for NK cell development.[36] The lin⁻ c-kit⁺ cells had much more abundant expression of Id2, PU.1, and SpiB1 mRNA compared with thymocytes (Figure 4). Note that mRNA of these transcription factors was decreased in the lin⁺ c-kit^{dim} cells, suggesting that they were at a later stage of differentiation than the lin⁻ c-kit⁺ population.

In addition to these transcription factors, we analyzed lymphotoxin α and β mRNA transcripts. Lymphotoxin α and β are reported to be critical for both NK cell development[37] and fulfillment of LTi functions.[38] The lin⁻ c-kit⁺ cells also had much more abundant mRNA transcripts of lymphotoxin α and β compared with thymocytes (Figure 4).

We next examined RAG-1, RAG-2, and pTα mRNA, which are essential for early T-cell differentiation. Although these transcripts were detectable in the lin⁻ c-kit⁺ cells, their expressions were far lower than that in thymocytes (Figure 4). These results indicate that the lin⁻ c-kit⁺ cells have an immature nature and the potential to differentiate into NK cells.

The lin⁻ c-kit⁺ LPMCs Are Committed to NK Cell Lineage In Vitro

Based on the results obtained so far, we assumed that the lin⁻ c-kit⁺ cells in the human adult intestine were a subset very close to T/NKPs. To confirm the differentiation capacity of the lin⁻ c-kit⁺ cells, we cultured LPMCs after depletion of both CD3⁺ and CD56⁺ cells without any exogenous stimuli. This culture method can maintain the interaction of the c-kit⁺ cells with the surrounding cells, via cell-cell contact or humoral soluble factors, which may be essential for the differentiation process. At the beginning of the culture period, we confirmed that the lin⁺ c-kit^{dim} subset was excluded completely because of CD3⁺ and CD56⁺ cell depletion (Figure 5*A*). However, surprisingly, c-kit^{dim} cells expressing lineage markers emerged and increased during the culture period (Figure 5*A* and *B*). Conversely, the lin⁻ c-kit⁺ cells gradually decreased. These lin⁺ c-kit^{dim} cells must have developed from the lin⁻ c-kit⁺ subset because the c-kit^{dim} cells did not emerge from the sorted c-kit⁻ population during 72 hours of culture (Supplementary Figure 1; supplementary material online at www.gastrojournal.org).

The c-kit⁺ cells became larger in size and had more granularity as they developed (Figure 5*C*). Most of the c-kit^{dim} cells up-regulated NK cell markers such as CD56, CD161, and IL-2Rβ, and they also expressed integrin α_E (Figure 5*C*, *D*, and *E*, Table 1). However, they did not express activated NK cell markers CD80 and CD86 (Table 1).[39] Meanwhile, very few CD3⁺ cells could be detected among the lin⁺ c-kit^{dim} populations (Figure 5*C* and *D*). Furthermore, the CD56⁺ cells in the newly emerging lin⁺ c-kit^{dim} cells contained cytotoxic granules (Figure 5*F*) and they could exert cytotoxicity against K562 cells (Figure 5*G*). They also were able to produce IFN-γ and TNF-α (Figure 5*H*). According to some previous studies, it takes up to 2 weeks for NK cell development from HSC in vitro culture.[40] Therefore, the lin⁻ c-kit⁺ subset likely included the population that already committed to NK cell lineage.

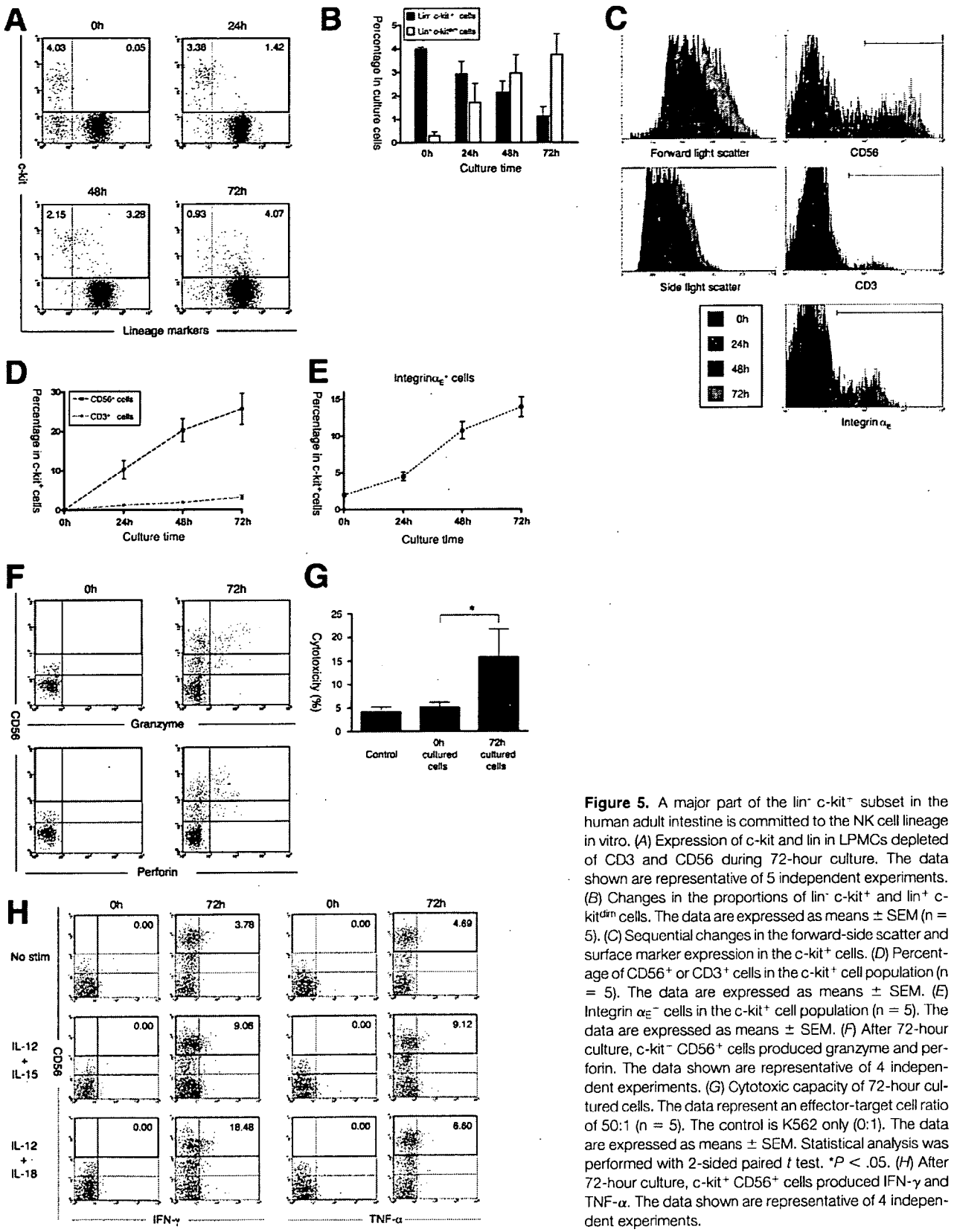

Figure 5. A major part of the lin$^-$ c-kit$^-$ subset in the human adult intestine is committed to the NK cell lineage in vitro. (*A*) Expression of c-kit and lin in LPMCs depleted of CD3 and CD56 during 72-hour culture. The data shown are representative of 5 independent experiments. (*B*) Changes in the proportions of lin$^-$ c-kit$^+$ and lin$^+$ c-kit^{dim} cells. The data are expressed as means ± SEM (n = 5). (*C*) Sequential changes in the forward-side scatter and surface marker expression in the c-kit$^+$ cells. (*D*) Percentage of CD56$^+$ or CD3$^+$ cells in the c-kit$^+$ cell population (n = 5). The data are expressed as means ± SEM. (*E*) Integrin α_E^- cells in the c-kit$^+$ cell population (n = 5). The data are expressed as means ± SEM. (*F*) After 72-hour culture, c-kit$^-$ CD56$^+$ cells produced granzyme and perforin. The data shown are representative of 4 independent experiments. (*G*) Cytotoxic capacity of 72-hour cultured cells. The data represent an effector-target cell ratio of 50:1 (n = 5). The control is K562 only (0:1). The data are expressed as means ± SEM. Statistical analysis was performed with 2-sided paired *t* test. $^*P < .05$. (*H*) After 72-hour culture, c-kit$^+$ CD56$^+$ cells produced IFN-γ and TNF-α. The data shown are representative of 4 independent experiments.

Table 1. Phenotypes of the Newly Emerging c-kit^{dim} Cells After 72-Hour In Vitro Culture

Cell surface markers	Cultured cells (72 h)
CD34	−
CD38	+++
CD33	++
CD2	+++
CD7	++
CD11b	+
CD11c	+
CD161	+++
CD94	+
NKG2D	+
CD158a/b	−
NKB1	−
L-selectin	−
CD80	−
CD83	+
CD86	−
CD209	−
IL-2Rα	++
IL-2Rβ	++
IL-3Rα	−/+
IL-7Rα	+++
IL-18Rα	+++
CCR7	+
CXCR3	+
CXCR5	−
CX3CR1	−
Integrin α_4	+++
Integrin β_7	+
Integrin α_E	+

−, 0%–5%; −/+, 5%–10%; +, 10%–50%; ++, 50%–75%; +++, 75%–100%.

When only isolated lin$^-$ c-kit$^+$ cells were rendered to in vitro culture, they lost viability with or without exogenous human cytokines such as IL-2 and/or IL-15. Then we performed transfer experiments in which RAG-2–deficient mice received isolated human lin$^-$ c-kit$^+$ LPMCs. Very surprisingly, 3 weeks after transplantation we could detect human lin$^-$ c-kit$^+$ cells exclusively in murine LPMCs but not in IELs or splenic lymphocytes (Figure 6*A*). The absence of CD56 expression indicated that they did not differentiate into NK cells in murine intestine. However, human CD56$^+$ cells emerged when murine LPMCs containing human lin$^-$ c-kit$^+$ cells were cultured with exogenous IL-2 and/or IL-15 (Figure 6*B*).

These results suggested that a large proportion of human LP lin$^-$ c-kit$^+$ cells were the NK cell precursors. Given that newly emerging lin$^+$ c-kit^{dim} cells from lin$^-$ c-kit$^+$ subtype shared a very similar phenotype with the lin$^+$ c-kit^{dim} cells that actually reside in human LPMCs (Figure 3B and Table 1), this differentiation process may actually occur in the human intestine.

LPMCs and IELs Contain Functional NK Cells

The results thus far have indicated that the lin$^-$ c-kit$^+$ cells in the intestine have the potential to differentiate into NK cells. There have been only a few reports on NK cells in the human intestine,[41,42] therefore, we examined CD56 expression on LPMCs and IELs. It revealed that a considerable number of CD3$^-$ CD56$^+$ cells certainly exist in LPMCs (Figure 7*A*). These CD3$^-$ CD56$^+$ cells, which are referred to as LPNKs, were larger and had more granular morphology than lamina propria T cells (Supplementary Figure 2; supplementary material online at www.gastrojournal.org). CD3$^-$ CD56$^+$ cells also were found in IELs, which are referred to as intraepithelial NK cells (IENKs) (Figure 7*A*).[42] We next compared surface marker expression among the lin$^-$ c-kit$^+$, lin$^+$ c-kit^{dim}, and intestinal NK cells (LPNKs and IENKs) (Figure 7*B*). NK cell markers such as CD94, CD161, and NKG2D increased in the following order: lin$^-$ c-kit$^+$ cells < lin$^+$ c-kit^{dim} cells < intestinal NK cells, which is consistent with CD56 up-regulation on lin$^+$ c-kit^{dim} cells. Conversely, immature cell markers such as c-kit, IL-7Rα, and CD33 were decreased in the same order. These changes in surface marker expression also were observed during differentiation of lin$^-$ c-kit$^+$ cells into lin$^+$ c-kit^{dim} cells (Table 1). Taken together, these results would support the hypothesis that lin$^-$ c-kit$^+$ cells differentiate into intestinal NK cells via lin$^+$ c-kit^{dim} cells, possibly at the site of the intestine.

It is known that PBNK cells can be divided into 2 subsets according to the intensity of CD56 expression: CD56^{dim} and CD56^{bright} NK cells.[43,44] Although CD56 expression on the intestinal NK cells was not as high as on CD56^{bright} NK cells, the intestinal NK cells were reminiscent of CD56^{bright} NK cells owing to the lack of CD16, CX3CR1, and killer cell inhibitory receptor (CD158a/b, NKB1) expression (Figure 7*B*).[45,46] Moreover, both the intestinal NK cells and the peripheral CD56^{bright} NK cells expressed CD33, whereas the peripheral CD56^{dim} NK cells did not (Figure 7*B*).

To confirm that the intestinal NK cells harbor NK functions, cytotoxic molecules were examined. Both LPNKs and IENKs contained granzyme and perforin; and they were equipped with cytotoxic function, although the activity was weaker than that in peripheral CD56^{dim} NK cells (Figure 7*C* and *D*). Both LPNKs and IENKs also produced IFN-γ and TNF-α at a level comparable with peripheral CD56^{bright} NK cells (Figure 7*E–H*). With these phenotypes (ie, lower expression of granzyme and perforin and higher IFN-γ and TNF-α production), intestinal NK cells are reminiscent of peripheral CD56^{bright} NK cells. However, they clearly were discriminated from peripheral CD56^{bright} NK cells in terms of CD83 and integrin α_E expression (Figure 7*B*). These unique characteristics of intestinal NK cells may support the idea that they may have an original in situ differentiation system independent from PBNKs.

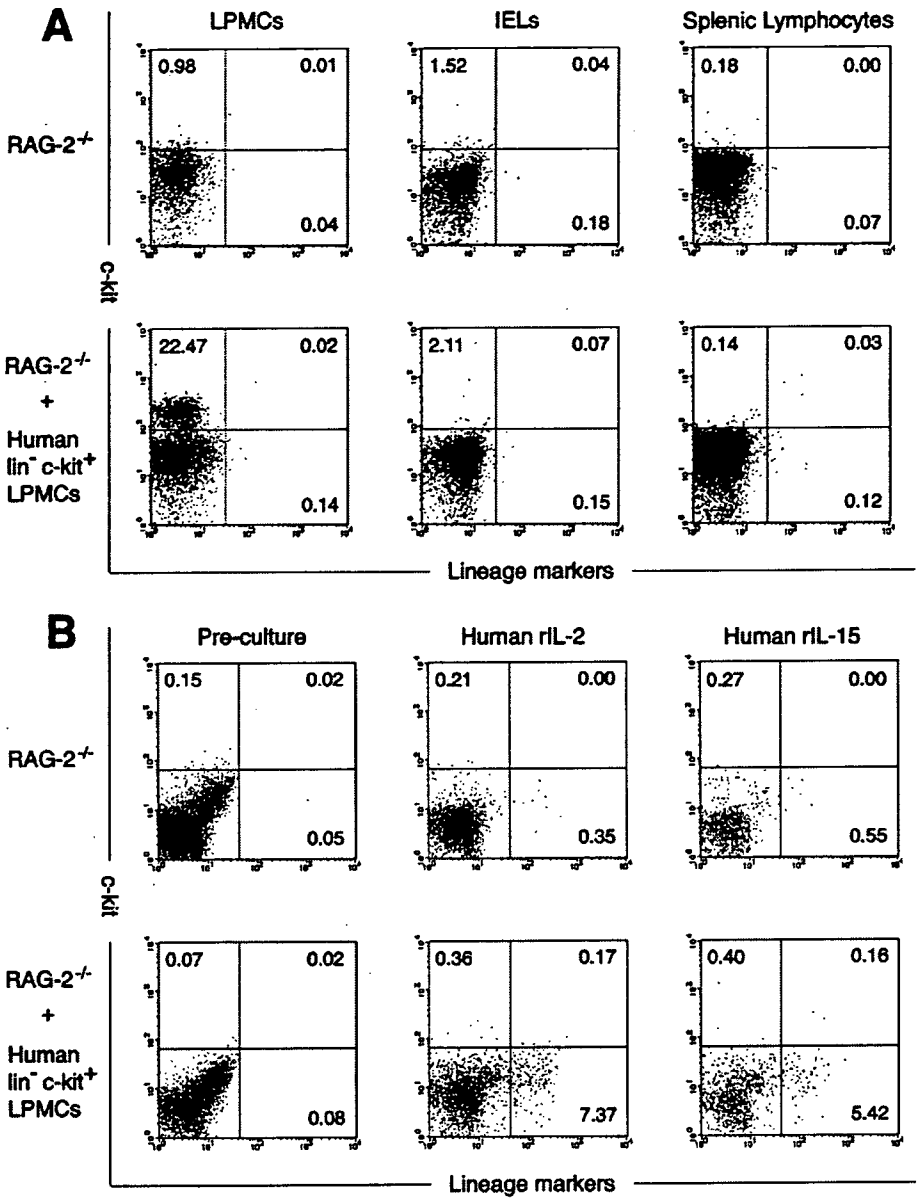

Figure 6. Human lin⁻ c-kit⁺ LPMCs after the transfer into recipient mice could differentiate into NK cells. (*A*) LPMCs, IELs, and splenic lymphocytes isolated from the RAG$^{-/-}$ mice transplanted with human lin⁻ c-kit⁺ LPMCs were stained by lineage markers and CD117 monoclonal antibody and were analyzed by fluorescence-activated cell sorter. The data shown are representative of 2 independent experiments. (*B*) Isolated LPMCs were cultured with human recombinant IL-2 (rIL-2) or rIL-15 for 7 days. The cultured cells were analyzed for expression of human CD3 and CD56. The data shown are representative of 2 independent experiments.

Intestinal NK Cells Are Increased in CD, Reflecting Accelerated Differentiation of lin⁻ c-kit⁺ Cells Into NK Cells

The involvement of NK cells in intestinal inflammation has not been well documented. Therefore, we examined intestinal NK cells in inflammatory bowel disease, a chronic inflammatory condition that consists of 2 major forms: CD and UC.[47] Flow cytometry revealed that both LPNKs and IENKs were increased in the samples from CD but not from UC patients, compared with

Figure 7. Analysis of surface antigen expression and function of intestinal NK cells. (*A*) LPMCs, IELs, and PBLs were stained for CD3 and CD56. CD3⁻ CD56⁺ cells were examined further for c-kit expression. (*B*) Expression of various surface markers, including NK cell markers, was compared among lin⁻ c-kit⁺ and lin⁺ c-kit^{dim} cells, LPNKs, IENKs, and PBNKs. The data shown are representative of more than 4 cases for each surface marker. (*C*) Production of granzyme, perforin from LPNKs, IENKs, and PBNKs were determined with intracellular staining. The data shown are representative of 4 independent experiments. (*D*) Cytotoxicity of freshly isolated LPNKs (n = 5) and PBNKs (n = 4). Effector-target ratio was 10:1. The data were expressed as means ± SEM. (*E*) IFN-γ and (*F*) TNF-α production from LPNKs (n = 5) and PBNKs (n = 4) after 72-hour culture with indicated cytokines. The data were expressed as means ± SEM. (*G*) IFN-γ or (*H*) TNF-α production in LPNKs, IENKs, and PBNKs after 8 hours of cytokine stimulation were detected using the Cytokine Secretion Assay Cell Detection Kit (Miltenyi Biotec). The data shown are representative of 4 independent experiments.

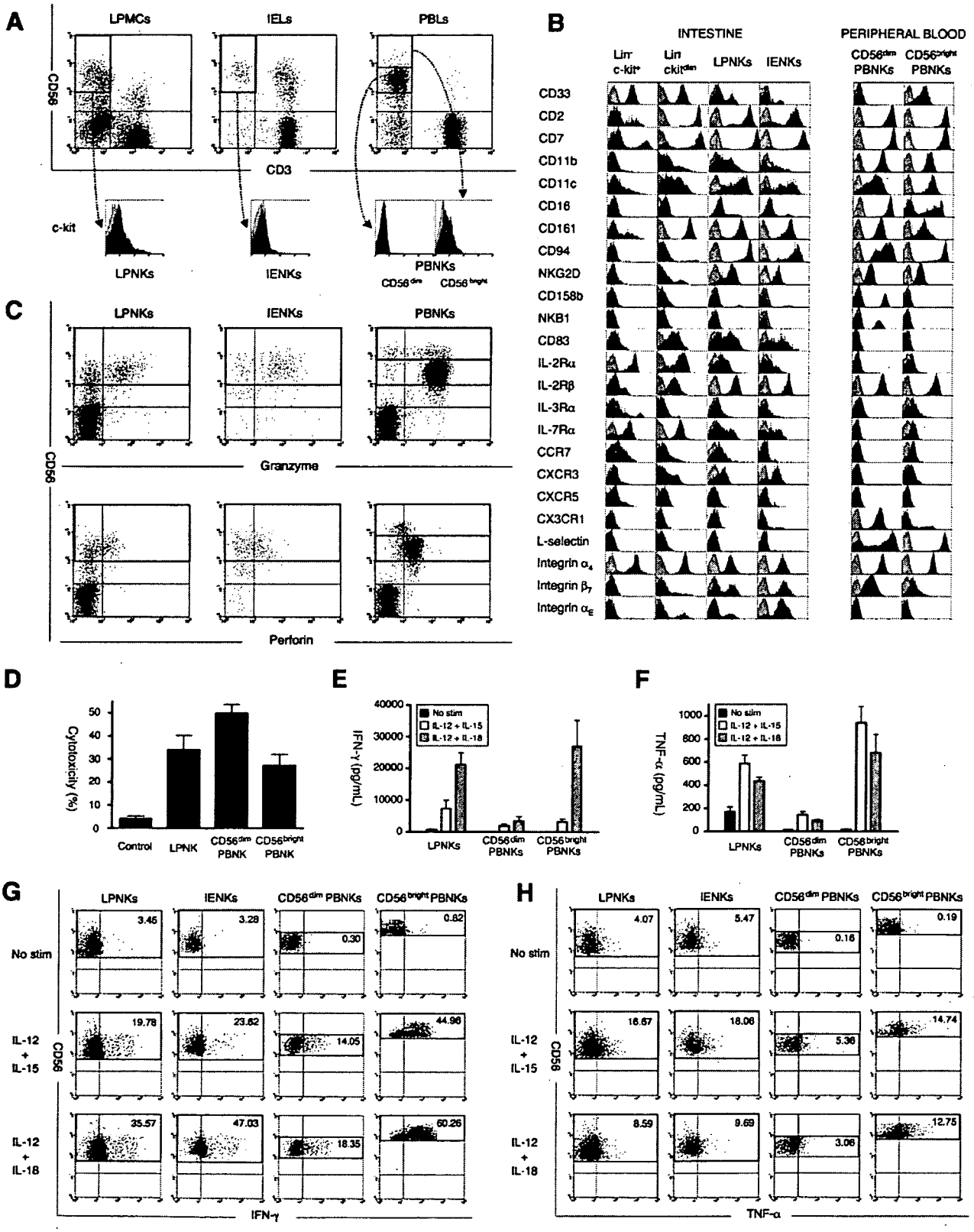
A
LPMCs
IELs
PBLs
CD56
CD3
c-kit
LPNKs
IENKs
PBNKs
CD56dim CD56bright
B
INTESTINE
PERIPHERAL BLOOD
Lin- c-kit+
Lin- ckitdim
LPNKs
IENKs
CD56dim PBNKs
CD56bright PBNKs
CD33
CD2
CD7
CD11b
CD11c
CD16
CD161
CD94
NKG2D
CD158b
NKB1
CD83
IL-2Rα
IL-2Rβ
IL-3Rα
IL-7Rα
CCR7
CXCR3
CXCR5
CX3CR1
L-selectin
Integrin α4
Integrin β7
Integrin αE
C
LPNKs
IENKs
PBNKs
CD56
Granzyme
Perforin
D
Cytotoxicity (%)
Control
LPNK
CD56dim PBNK
CD56bright PBNK
E
IFN-γ (pg/mL)
No stim
IL-12 + IL-15
IL-12 + IL-18
LPNKs
CD56dim PBNKs
CD56bright PBNKs
F
TNF-α (pg/mL)
G
No stim
IL-12 + IL-15
IL-12 + IL-18
3.45
3.28
0.30
0.82
19.78
23.62
14.05
44.96
35.57
47.03
18.35
60.26
IFN-γ
H
4.07
5.47
0.16
0.19
16.67
18.06
5.36
14.74
8.59
9.69
3.06
12.75
TNF-α

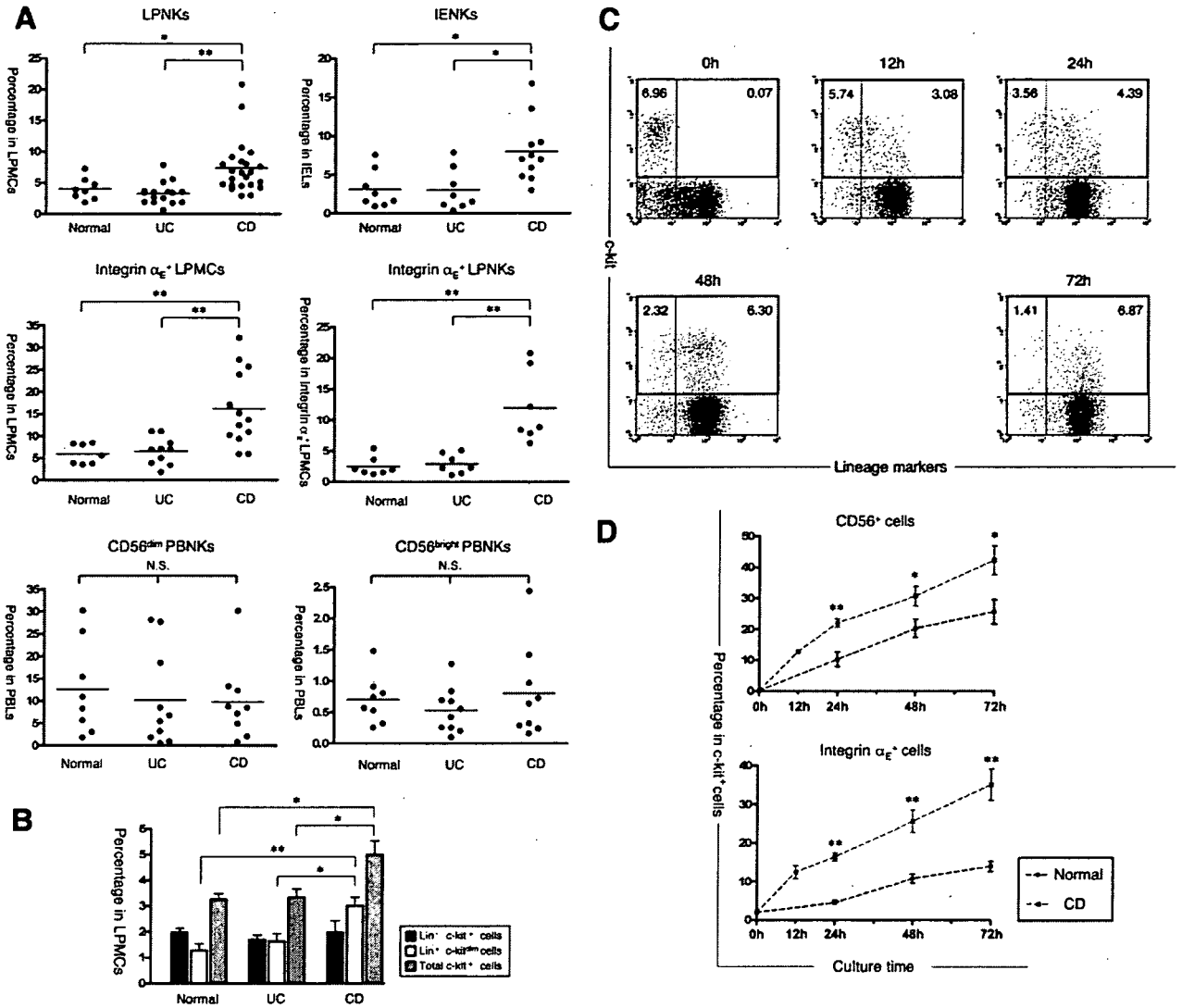

Figure 8. The c-kit^{dim} cells, LPNKs, and IENKs are increased in CD. (*A*) Percentage of NK cells among LPMCs (normal, n = 10; UC, n = 17; CD, n = 23) or IELs (normal, n = 8; UC, n = 8; CD, n = 11) (upper panels). Percentage of integrin $\alpha_E\beta_7^+$ cells among LPMCs (normal, n = 7; UC, n = 10; CD, n = 13) or LPNKs (normal, n = 7; UC, n = 7; CD, n = 7) (middle panels). Percentage of CD56^{dim} CD16$^+$ and CD56^{bright} CD16$^-$ NK cells among PBLs (normal, n = 8; UC, n = 10; CD, n = 9) (bottom panels). Statistical analysis was performed with the Kruskal–Wallis 1-way analysis of variance, and the Bonferroni–Dunn test for multiple comparisons. $^*P < .05$, $^{**}P < .01$. (*B*) Percentage of total c-kit$^+$, lin$^-$ c-kit$^+$, or lin$^+$ c-kit^{dim} cells among LPMCs (normal, n = 10; UC, n = 11; CD, n = 15). Results are expressed as means ± SEM. Statistical analysis was performed with the Kruskal–Wallis 1-way analysis of variance, and the Bonferroni–Dunn test for multiple comparisons. $^*P < .05$, $^{**}P < .01$. (*C*) LPMCs depleted of CD3 and CD56, obtained from CD patients, were cultured for 72 hours and analyzed for expression of c-kit and lin. The data shown are representative of 7 independent experiments. (*D*) The line graph shows the time–course changes for CD56+ or integrin α_E^+ cells in c-kit$^+$ LPMCs from normal controls (n = 5) or CD patients (n = 7). The data are expressed as means ± SEM for the percentage of CD56$^+$ or integrin α_E^+ cells among the c-kit$^+$ cells. Statistical analysis was performed with a 2-sided Mann–Whitney *U* test. $^*P < .05$, $^{**}P < .01$.

normal controls (Figure 8*A*). In contrast, the frequency of NK cells, both for CD56^{dim} and CD56^{bright}, was similar in peripheral blood among the 3 groups (Figure 8*A*). Furthermore, although lin$^-$ c-kit$^+$ cells existed with similar frequency, the lin$^+$ c-kit^{dim} cells were increased significantly in CD compared with UC or normal controls (Figure 8*B*). Then we repeated the in vitro culture experiments shown in Figure 5 and found that more lin$^+$ c-kit^{dim} cells were detected in CD samples at each time point (Figure 8*C*), and the majority of these cells expressed CD56 and integrin α_E (Figure 8*D*). Taken together, the increase of LPNKs and IENKs in CD patients could have been owing to accelerated differentiation from lin$^-$ c-kit$^+$ cells. Given that the intestinal NK cells can strongly produce IFN-γ and TNF-α, which is a key cytokine in the pathogenesis of CD, these increased intestinal NK cells may play a pathogenic role in chronic inflammation in CD.

Discussion

The sites of NK cell development in adults are understood poorly.[40,48] Although T/NKPs have been identified only in fetal tissues, the bone marrow is presumed to be the main site of NK cell generation in adults.[40,48] In this study, we have shown that lin$^-$ c-kit$^+$ cells in human adult intestine could differentiate into c-kit^{dim} cells, which express CD56 during in vitro culture, suggesting that these cells are NK cell precursors. Moreover, further analysis showed that in vitro differentiated c-kit^{dim} CD56$^+$ cells seemed to correspond to c-kit^{dim} CD56$^+$ cells actually present in human adult intestine. Combined together, adult intestine may have unique NK cell differentiation system in which lin$^-$ c-kit$^+$ NK precursors undergo in situ differentiation via c-kit^{dim} cells.

The newly discovered c-kit$^+$ cells in the human adult intestine also express CD34, another marker for HSCs or immune precursor cells.[17,28] In addition to c-kit and CD34, the intestinal immune precursors expressed CD38^{dim}, CD44, CD45RA, and Thy-1, the phenotypes of which correspond to those of common lymphoid progenitors or T/NKPs.[49] Furthermore, they had abundant mRNA transcripts for Id2, PU.1, SpiB1, and lymphotoxin, all of which are essential for HSC differentiation or NK cell development.

In the murine intestine, c-kit–expressing cells form small clusters named CP.[8] It has been reported that CP cells have the potential to differentiate mainly into extrathymic T cells in the intraepithelial space.[10] Interestingly, the intestinal c-kit$^+$ immune precursor cell expression level of RAG mRNA was very low, and the RAG expression level was similar to CP cells, which was reported previously by Oida et al.[50] Recent studies have shown that CD3$^-$ CD7$^+$ cells in the human fetal intestine express pTα mRNA[13] and give rise to CD3$^+$ T cells in vitro and in vivo, using SCID mice with engrafted human fetal intestine.[14] The intestinal c-kit$^+$ immune precursor cells are also CD3$^-$ CD7$^+$ and express RAG-1, RAG-2, and pTα mRNA. These results imply that the immune precursor cells in adult intestine include a subset similar or identical to the CD3$^-$ CD7$^+$ cells in the fetal intestine and they may differentiate into T cells in unusual environment, such as lymphopenia. However, in that they do not form aggregates and are much more committed to NK cells rather than T cells, they should be distinguished from the murine CP cells that differentiate into intraepithelial T cells. On the other hand, a recent study showed that c-kit$^+$ cells in CP represent LTi in adult mice, which organize isolated lymphoid follicles.[12] Furthermore, because LTi and T/NKPs have similar expression patterns of surface antigens and transcription factors,[51,52] they are considered to be subsets that are related closely to each other. Given that intestinal immune precursor cells also are similar to LTi in terms of surface antigen expression and transcriptional profile, it is possible that they contain an adult LTi subset.

Little information is available about intestinal NK cells. An earlier article reported on lymphokine activated killer activity in human LPMCs,[53] although they failed to identify NK cells in LPMCs, possibly because of the lack of suitable NK cell markers at that time. Some recent reports showed that human LPMCs and IELs contain NK cells capable of killing tumor cells and producing several cytokines, such as IFN-γ and TNF-α.[41,43] In this study, we intensively examined the intestinal NK cells to verify the hypothesis that they develop in situ from the immune precursor cells in intestinal lamina propria. In terms of NK cell markers, expression of CD56, as well as CD94, CD161, and NKG2D, was lowest in the c-kit$^+$ cells, and inversely highest in LPNKs/IENKs. In contrast, immature cell markers such as c-kit, IL-7Rα, and CD33 were highest in the intestinal immune precursor cells. Furthermore, these changes in surface marker expression also were observed during in vitro differentiation of lin$^-$ c-kit$^+$ cells into c-kit^{dim} cells. Collectively, these results support the idea that intestinal immune precursor cells can give rise to intestinal NK cells via c-kit^{dim} NKP-like cells.

PBNKs can be classified into 2 subsets. One subset is the conventional CD56^{dim} NK cells and the other is the CD56^{bright} NK cells.[43,44] Absence of CD16 expression is also a characteristic feature of the CD56^{bright} NK cells. Although CD56 expression of the intestinal NK cells was not as high as the peripheral CD56^{bright} NK cells, absence of CD16 expression indicates a similarity between the intestinal NK cells and the peripheral CD56^{bright} NK cells. In addition, we found that both the intestinal NK cells, especially LPNKs, and peripheral CD56^{bright} NK cells expressed CD33. Although CD33 is a myeloid lineage marker, it is reported that CD33$^+$ CD34$^+$ HSCs can give rise to CD16$^-$ NK cells in vitro.[54] Given that most intestinal immune precursor cells express CD33, and that intestinal NK cells are CD33$^+$ CD16$^-$, it is reasonable to assume that the intestinal NK cells may originate from the immune precursor cells. Furthermore, CD33 is reported to be expressed on CD56^{bright} NK cells in umbilical cord blood[55] and on T/NKPs in the fetal thymus.[29] Although the origin of CD56^{bright} NK cells still is controversial, it recently was reported that the peripheral CD56^{bright} NK cells differentiate in the lymph nodes, unlike conventional CD56^{dim} NK cells.[56] CD33$^+$ CD16$^-$ may be a phenotype that characterizes NK cells developing outside the bone marrow, such as lymph nodes, the thymus, and maybe the intestine.

The pathophysiologic contribution of intestinal NK cells to inflammatory bowel disease has yet to be elucidated. An interesting recent report suggested that the intestinal NK cells maintain homeostasis of intestinal mucosal immune system in mice. However, their roles have not been resolved in human beings.[57] We found that the differentiation of the intestinal immune precursor cells into NK cells was accelerated in CD, resulting in an increase in the number of intestinal NK cells in CD